

Adiabatic gauge potential and signatures of quantum criticality

A THESIS
SUBMITTED FOR THE DEGREE OF
MASTER OF PHYSICS

by

Pritam Sarkar

Under supervision of
Prof. Parthasarathi Majumdar

And with guidance from
Prof. Arnab Sen



SCHOOL OF PHYSICS SCIENCE
INDIAN ASSOCIATION FOR THE CULTIVATION OF SCIENCE
KOLKATA - 700032, INDIA

MAY 2024

To Whom It May Concern

This is to certify that the compilation of **10th Semester's Project-Report** titled **Adiabatic gauge potential and signatures of quantum criticality**, submitted by **Pritam Sarkar** (Roll No.:2019/UG/038, SPS), has been compiled under the supervision of the undersigned in the School of Physical Sciences, Indian Association for the Cultivation of Science, Kolkata, 700032, as a requirement of the BS-MS Program in Physics.

Prof. Parthasarathi Majumdar

Indian Association for the Cultivation of Science

Date:

© Pritam Sarkar
May 2024
All rights reserved

This thesis is dedicated to
all those wonderful human beings who opened up
new windows of perception to me.

Acknowledgement

I am deeply thankful to Prof Parthasarathi Majumdar for making sure that *with my heart in one place, I do not do something else* to push towards my interests in statistical mechanics, and Prof. Arnab Sen who very generously allowed me this opportunity to roam a little wildly, in a land very elegant yet much less explored.

Several discussions with my friends Arjo Dasgupta and Adhiraj Talukdar has clarified many intricacies of the topic which have been very pleasant and helpful.

Moreover I am also highly grateful to Prof. Subhabrata Das from the department of Mathematics at the Presidency University, for helping me understand many nuances related to riemannian metric and existence-uniqueness of embedded surfaces that have the same intrinsic distances as the one with the metric.

Contents

1	Introduction	1
2	Adiabatic gauge potential (AGP)	2
2.1	Co-moving frame	2
2.1.1	Relation with Berry phase	4
2.1.2	A formula for solving AGPs	4
2.2	A variational principle for AGPs	4
2.2.1	Dissipationless protocols	5
3	Transitionless quantum drives	7
3.1	Counter-diabatic hamiltonian	8
3.1.1	Transitionless evolution of classical spin trajectories	9
3.2	A transitionless LZM problem	10
3.2.1	A reverse-reverse engineering perspective	10
4	AGP for many-body systems	13
4.1	XY Spin- $\frac{1}{2}$ chain with transverse magnetic field (XYTF)	13
4.1.1	Derivation using the variational principle	14
4.2	AGP for the ground state	15
5	A geometric perspective of quantum information	16
5.1	Fidelity susceptibility	16
5.2	Ground state manifold (GSM)	18
5.2.1	Intrinsic geometry of quantum phases of matter	19
5.2.2	Ground state manifold of XYTF model	20
5.2.3	Scalar curvature and Euler-characteristics of XYTF	28
5.2.4	Discussions	28
6	A susceptibility of entanglement-entropy	31
6.1	Exact results for XY spin chain in transverse magnetic field :	32
6.1.1	Signature of quantum criticality in finite XY model	34
6.1.2	Signature of quantum criticality in finite TFIM	35
7	Summary and open ends	37
8	Conclusion	38
9	Prospects and future directions	39

List of Figures

3.1	Transitionless driving field for $\gamma = 2.5$	12
3.2	Transitionless driving field for $\gamma = 1$	12
4.1	$\alpha_l(h)$: point of view - A	14
4.2	$\alpha_l(h)$: point of view - $A_{\text{antipodal}}$	14
5.1	Phase Diagram of Quantum XY Chain with Anisotropy (γ) and under Transverse Magnetic Field (h)	17
5.2	non-trivial poles in the integrands of geometric tensor components when $L \rightarrow \infty$	21
5.3	for $ h < 1$ [<i>Blue</i>], & $h > 1$ [<i>Red</i>]	23
5.4	for $ h < 1$ [<i>Blue</i>], & $h < -1$ [<i>Orange</i>]	23
5.5	$(\gamma - \phi)$ plane when $ h < 1$	24
5.6	$(\gamma - \phi)$ plane when $ h > 1$	24
5.7	Conformally Flat $(h - \gamma)$ -cut for $ h < 1$	26
5.8	Exact $(h - \gamma)$ -cut for $ h < 1$	26
5.9	K for $(\phi - h)$ Plane for fixed γ	29
5.10	K for $(\phi - \gamma)$ Plane for fixed h	29
5.11	K for $(h - \gamma)$ Plane	29
5.12	K for the full parameter space	29
6.1	Examples of $\langle \sigma^z \rangle$ for different system sizes when $\gamma = 1$	33
6.2	Examples of $\langle \sigma^z \rangle$ for different system sizes when $h = 0$	33
6.3	Susceptibility of Entanglement-Entropy $\Xi_{\gamma\gamma}^{(h=0)}$ for XY model	34
6.4	Scaling of $ \gamma_c^{L \rightarrow \infty} - \gamma_c^{\text{finite } L} $ w.r.t. $\frac{1}{L}$ for XY model in the Log-Log scale	34
6.5	Susceptibility of Entanglement-Entropy $\Xi_{hh}^{(\gamma=1)}$ for Transverse Field Ising model	35
6.6	Scaling of $ h_c^{L \rightarrow \infty} - h_c^{\text{finite } L} $ w.r.t. $\frac{1}{L}$ for Transverse Field Ising model in the Log-Log scale	35

Chapter 1

Introduction

For time dependent problems there are time-dependent parameters within some underlying hamiltonian $H_0(\lambda(t))$, and in general due to arbitrary variation of the parameters, the actual dynamical spectrum of the evolving systems may vary drastically from the instantaneous eigenspectrum at every timestamp. Gauge potentials in this context are the generators of the canonical transformations $q(\lambda)$ and $p(\lambda)$ which leave the hamiltonian invariant. In particular, the adiabatic gauge potentials ensure that the hamiltonian corresponding to coupling $\lambda' = \lambda + \delta\lambda$ in new coordinates q', p' "commutes", i.e., has vanishing Poisson bracket, with the hamiltonian corresponding to coupling λ in the original coordinates q, p . Such special canonical transformations in classical systems are analogous to special unitary transformations in quantum systems which diagonalize the instantaneous hamiltonian. The vanishing Poisson brackets in classical systems then correspond to vanishing commutator between two diagonal matrices representing the instantaneous diagonalized hamiltonian in quantum systems.

The study of adiabatic gauge potentials offers numerous advantages, as it has many ramifications and practical applications - notably in controlling quantum transitions and devising transtitionless drives with rapid change of parameters; pivotal for maintaining quantum coherence.

These potentials facilitate counterdiabatic driving, which is instrumental in emulating adiabatic dynamics without the need for slow parameter changes, a boon for rapid quantum state-manipulation. Furthermore, they allow for an algebraic determination of explicit forms of the adiabatic gauge potentials, easing their application across various quantum systems. Crucially, they also enable a geometric characterization of quantum phases within the parameter space, endowing a non-euclidean metric in the parameter space of a general Many-Body Quantum System. This encapsulates the information of statistical distinguishability of the ground states of the system. Geometric aspect not only enriches the theoretical framework but also serves as a sophisticated tool for detecting and analysing quantum phase transitions, providing a **deeper insight into the Structure of the Spectrum of a Time-Dependent System**. In the rest of report, Adiabatic Gauge Potentials will be mentioned as AGP for brevity.

Furthermore, motivated from classical information theory, a susceptibility of entanglement-entropy has been proposed that generalises into an infinite class of riemannian metric tensors encapsulating the information contained in entanglement-entropy using only density matrices. It is demonstrated that this quantity exhibits prominent signature of quantum criticaity, that emerges only in thermodynamically large systems, even in small finitely many systems - asymptotically reaching to the desired thermodynamic result. Its peak converges to the thermodynamic critical point with power-law scaling w.r.t. the system sizes as demonstrated in transverse field Ising model and XY model of spin- $\frac{1}{2}$ chains.

Chapter 2

Adiabatic gauge potential (AGP)

Key Aspects: *Gauge Potentials are generators of translation in Parameter Space. Adiabatic gauge potentials are a special subset of these which diagonalize the instantaneous hamiltonian, attempting to leave its eigenbasis invariant as the parameter is changed. These adiabatic gauge potentials generate non-adiabatic corrections to the hamiltonian in the moving frame.*

It has parallel development from generators of canonical transformation in classical hamiltonian mechanics, that which generalizes generator of unitary transformation in quantum mechanics - something that is fundamental to understand the effect of time-dependence in arbitrary systems, but that direction has not been pursued in this project. The discussions made here involve particularly closed quantum systems, where the non-diagonalizability of Hamilton for different timestamps for time-dependent problem, is addressed in depth.

Consider a family of mamiltonians $\mathcal{H}(\lambda(t))$, dependent on a continuous parameter(s) $\lambda(t)$. These are assumed to be non-singular and smoothly differentiable. For each $\lambda(t)$, the hamiltonian is diagonalized by a set of eigenstates $|m(\lambda(t))\rangle$, termed the adiabatic basis. When the parameters $\lambda(t)$ are varied according to adiabatic (extremely slow) changes, the adiabatic theorem asserts that these states are connected through the theorem's application. Assuming non-degenerate eigenstates, the adiabatic states are unique except for a possible phase factor.¹ These states are linked by a specific unitary transformation, and the corresponding gauge potentials are known as *adiabatic gauge potentials*. These gauge potentials possess several properties that will be utilized subsequently. There has been numerous development in the literature on such ideas but with different names and very different approaches [1], [2]. Shortcut to Adiabaticity, Transitionless Quantum Drive and Counter-diabatic drive are the most notable terms associated with this exact same idea. As Berry [2] demonstrates this idea particularly for many body spin-systems, Polkovnikov et al. [1] develops the picture for general setting.

2.1 Co-moving frame

Consider there is a $H_0(\lambda(t))$ and the unitary transformation U_λ that diagonalizes the instantaneous hamiltonian at every timestamps. Since $H_0(\lambda(t))$ is a family of hermitian matrices parameterized by t , at every single instance of time t , the corresponding hamiltonian will have a spanning eigenspectrum, so construct a family of unitary operators $\{U\}_{\lambda(t)}$ where the elements are U_λ , which diagonalizes the hamiltonian. The **Co-Moving Frame** here is defined to satisfy -

$$|\tilde{\psi}(t)\rangle = U_\lambda^\dagger |\psi_\lambda(t)\rangle \quad \& \quad \partial_\lambda(|\tilde{\psi}(t)\rangle) = 0 \quad (2.1)$$

¹An adiabatic basis can be defined more broadly as a set of eigenstates that are adiabatically connected, meaning that they evolve coherently with an infinitesimal change of the parameter(s) $\lambda(t)$. For instance, if two levels intersect, they may reorder energetically, yet maintain their adiabatic connection, remaining non-singular.

meaning that the parameters do not change in the co-moving Frame, maintaining the consistency with known intuition from classical physics about comoving frames. Now that we understand the idea of co-moving frame in quantum mechanics we wish to know what hamiltonian drives these solutions of time-dependent problem exactly? Or in other words, **we want the hamiltonian that causes evolution of the co-moving frames w.r.t. the Schrodinger Eq, i.e.**

$$\begin{aligned} i\hbar \partial_t |\tilde{\psi}(t)\rangle &= i\hbar \partial_t (U_\lambda^\dagger |\psi_\lambda(t)\rangle) = i\hbar [(\partial_t U_\lambda^\dagger) |\psi_\lambda\rangle + U_\lambda^\dagger \partial_t |\psi_\lambda(t)\rangle] \\ &= [U_\lambda^\dagger H_0 U_\lambda - i\hbar U_\lambda^\dagger (\partial_t U_\lambda)] |\tilde{\psi}(t)\rangle = \tilde{H}_m |\tilde{\psi}(t)\rangle \end{aligned} \quad (2.2)$$

Note that throughout the report, the tilde notation mean everything regarding the comoving frame, and the other one for Lab frame or instantaneous basis of the hamiltonian. This gives that, in the co-moving frame the hamiltonian is² :

$$\tilde{H}_m = U_\lambda^\dagger H_0 U_\lambda - i\hbar U_\lambda^\dagger (\partial_t U_\lambda) = U_\lambda^\dagger H_0 U_\lambda - \dot{\lambda} (i\hbar U_\lambda^\dagger (\partial_\lambda U_\lambda)) \quad (2.3)$$

Where $U_\lambda^\dagger H_0 U_\lambda$ is diagonal by construction, and the other contribution is due to the $(i\hbar U_\lambda^\dagger \partial_t U_\lambda)$ term, which makes \tilde{H}_m a non-diagonal operator - **meaning that the transition between states, during time-evolution are only caused by the term $(i\hbar U_\lambda^\dagger \partial_\lambda U_\lambda)$ because $[\tilde{H}_m(\lambda(t)), \tilde{H}_m(\lambda(t'))] = \dot{\lambda}^2 [\tilde{A}(\lambda(t)), \tilde{A}(\lambda(t'))]$ in the comoving frame.**

Now getting back to the basic ideas about generators of unitary transformations, denote $\tilde{\mathcal{A}}_\lambda$ to be the generator of U_λ . This means

$$i\hbar \partial_\lambda U = \tilde{\mathcal{A}}_\lambda U_\lambda \implies \tilde{\mathcal{A}}_\lambda = i\hbar U_\lambda^\dagger (\partial_\lambda U_\lambda) \quad (2.4)$$

This is the gauge potential associated with change of parameters, evaluated in the comoving frame. Note that for every operator \mathcal{O} that acts on the lab-frame, $\tilde{\mathcal{O}} = U_\lambda^\dagger \mathcal{O} U_\lambda$ acts on the comoving frame. Therefore the Gauge Potential in the lab frame becomes

$$\mathcal{A}_\lambda = U_\lambda \tilde{\mathcal{A}}_\lambda U_\lambda^\dagger = i\hbar (\partial_\lambda U_\lambda) U_\lambda^\dagger \quad (2.5)$$

Now notice something interesting here:

$$\begin{aligned} \hat{\mathcal{A}}_\lambda |\psi_\lambda(t)\rangle &= i\hbar (\partial_\lambda U_\lambda) (U_\lambda^\dagger |\psi_\lambda(t)\rangle) = i\hbar (\partial_\lambda U_\lambda) |\tilde{\psi}(t)\rangle \\ &= i\hbar [\partial_\lambda (U_\lambda |\tilde{\psi}(t)\rangle) - U_\lambda \cancel{\partial_\lambda |\tilde{\psi}(t)\rangle}] = i\hbar \partial_\lambda |\psi_\lambda(t)\rangle \end{aligned} \quad (2.6)$$

Meaning that -

$$\hat{\mathcal{A}}_\lambda \equiv i\hbar \partial_\lambda \quad \text{In the Lab Frame} \quad (2.7)$$

This solidifies the interpretation of such gauge potentials as generators of translation in the space of all parameters. Therefore, whenever any of the parameter λ evolves under time, i.e. $\dot{\lambda} \neq 0$, then the **co-moving hamiltonian** \tilde{H}_m has nontrivial contributions from the time dependence in the parameters of the theory due to the second term in it.

With these ideas in mind, we can rewrite the co-moving hamiltonian in the following form:

$$\tilde{H}_m = U_\lambda^\dagger H_0 U_\lambda - \dot{\lambda} \tilde{\mathcal{A}}_\lambda \quad (2.8)$$

This puts us in the context of co-moving frames, as it helps understanding an essential aspect of time-dependent problems; which is to find a frame, where the variance of the parameters are frozen - which is equal to saying $\partial_\lambda (|\tilde{\psi}(t)\rangle) = 0$.

²This is the consistency condition for the exact dynamically evolving states to be the comoving states of the original time-dependent problem

2.1.1 Relation with Berry phase

It is important to note that the diagonal elements of the adiabatic gauge potential in the basis of $\mathcal{H}(\lambda)$ are, by definition, the Berry connections:

$$A_\lambda^{(n)} = \langle n(\lambda) | A_\lambda | n(\lambda) \rangle = i\hbar \langle n(\lambda) | \partial_\lambda | n(\lambda) \rangle. \quad (2.9)$$

Where, if we consider some circuit in the parameter space³ such that its endpoints match, then there will be an accumulated phase depending on the topology of the region enclosed by the circuit, i.e. whether that is simply connected or not. This phase factor can be determined by

$$\gamma_n = \oint_{\text{circuit}} A_\lambda^{(n)} d\lambda \quad (2.10)$$

Which is the famous Berry Phase.

2.1.2 A formula for solving AGPs

Our goal is to address the effect of such gauge potentials for general time-dependent problems. It should be noted that the gauge potential, up to a sign, is essentially the hamiltonian, and its expected value inversely relates to energy. A key property of these gauge potentials is revealed upon differentiation with respect to the parameter λ . It is easy to find the following things after a little algebra.

$$\langle m | \mathcal{A}_\lambda | n \rangle = \frac{i}{\hbar} \frac{\langle m | \partial_\lambda \mathcal{H} | n \rangle}{E_m - E_n} \quad (2.11)$$

$$\implies i\hbar \partial_\lambda \mathcal{H} = [\mathcal{A}_\lambda, \mathcal{H}] - i\hbar \mathcal{M}_\lambda, \quad \text{Where} \quad \mathcal{M}_\lambda = - \sum_n \frac{\partial E_n(\lambda)}{\partial \lambda} |n(\lambda)\rangle \langle n(\lambda)| \quad (2.12)$$

is a diagonal operator in the energy eigenbasis, representing generalized forces corresponding to different eigenstates of \mathcal{H} . From the above and considering that $[\mathcal{H}, \mathcal{M}_\lambda] = 0$, the adiabatic gauge potentials fulfill:

$$[\mathcal{H}, i\hbar \partial_\lambda \mathcal{H} - [\mathcal{A}_\lambda, \mathcal{H}]] = 0. \quad (2.13)$$

This equation can be used to find the adiabatic gauge potentials directly without need of diagonalizing the hamiltonian.[1]

2.2 A variational principle for AGPs

The principal idea is that adiabatic gauge potentials can be derived via a minimization principle, which subsequently facilitates the formulation of variational approaches to obtain approximate gauge potentials. These variational constructs prove instrumental in devising *counter-diabatic strategies*. As shown before, adiabatic gauge potentials may become singular when the energy spectrum has any gap, coupled with non-negligible matrix elements of the generalized force operator $-\partial_\lambda \mathcal{H}$ among adjacent eigenstates - a scenario termed as the 'small denominator problem'. While such divergences at discrete points like phase transitions are manageable, in chaotic systems, they necessitate nuanced regularization. The crux of the complication stems from the exact adiabatic gauge potentials' capacity to trace both the information of phases away from the gap but also arbitrarily near to it.

While Eqs. (13) defining the AGP cannot always be solved exactly, they can be used to derive a useful and tractable variational ansatz for general, time-dependent problems. To do so, let us begin by reformulating these equations as a **minimum action principle**, which serves as a seed for developing efficient approximate schemes. We will focus our derivation on the more general case of quantum systems, keeping in mind that in the classical limit one simply has to substitute the commutators with poisson brackets and traces of operators with averages over classical phase space.

³essentially just a curve

Define the hermitian operator $G_\lambda(x)$ as

$$G_\lambda(\chi) = \partial_\lambda \hat{H} + \frac{i}{\hbar} [\chi, \hat{H}], \quad (2.14)$$

where the argument χ is itself a hermitian operator. Then Eq. (12) determining the adiabatic gauge potential \hat{A}_λ , simply reads $G_\lambda(\hat{A}_\lambda) = -\hat{M}_\lambda$.

Instead of directly solving for $\chi = \hat{A}_\lambda$, we may reformulate it as a problem of minimization the operator distance between $G_\lambda(\chi)$ and $-\hat{M}_\lambda$, with respect to χ . Since G_λ is linear in χ it is natural to use the Frobenius norm for defining the distance, i.e.,

$$D^2(\chi) = \text{Tr} \left[\left(\partial_\lambda \hat{H} + \frac{i}{\hbar} [\chi, \hat{H}] + \hat{M}_\lambda \right)^2 \right] = \text{Tr}[G_\lambda(\chi)^2] + \text{Tr}[\hat{M}_\lambda^2] + 2\text{Tr}[G_\lambda(\chi) \hat{M}_\lambda]. \quad (2.15)$$

Clearly the distance is indeed minimal (zero) when $G_\lambda = -\hat{M}_\lambda$. Tracing in the energy eigenbasis and using cyclic properties of the trace, one finds

$$\text{Tr}(M_\lambda G_\lambda) = \text{Tr}(M_\lambda \partial_\lambda \hat{H}) + \frac{i}{\hbar} \text{Tr}(M_\lambda [\chi, \hat{H}]) = -\text{Tr}(\hat{M}_\lambda^2) - \frac{i}{\hbar} \text{Tr}([\hat{M}_\lambda, \chi]) \quad (2.16)$$

$$D^2(\chi) = \text{Tr}[G_\lambda(\chi)^2] - \text{Tr}[\hat{M}_\lambda^2], \quad (2.17)$$

where we used that the operator \hat{M}_λ commutes with \hat{H} and that $\text{Tr}(\hat{M}_\lambda \partial_\lambda \hat{H}) = -\text{Tr}(\hat{M}_\lambda^2)$, which becomes obvious if we explicitly write the trace in the eigenbasis of the hamiltonian. Since the generalized force term does not depend on χ , it does not affect the extremization w.r.t. χ . Hence, minimizing the distance is equivalent to minimizing the norm of G_λ . One can thus consider the norm of G_λ , as the action associated with the gauge potential:

$$S[\chi] = \text{Tr}[G_\lambda(\chi)^2] \quad (2.18)$$

It can easily be minimized by expanding x in some operator basis. The distance is minimized whenever \hat{A}_λ satisfies:

$$\left. \frac{\delta S}{\delta \chi} \right|_{\chi=\hat{A}_\lambda} = 0 \quad \Rightarrow \quad [\hat{H}, \partial_\lambda \hat{H} + \frac{i}{\hbar} [\hat{A}_\lambda, \hat{H}]] = 0 \quad (2.19)$$

A more straightforward approach to understanding that $\chi = \hat{A}_\lambda$ optimizes the distance between $G_\lambda(\chi)$ and M_λ is to recognize that within the eigenbasis of H , the diagonal components of G_λ are independent of χ . Thus, by targeting the norm of G_λ , we effectively reduce the sum of its off-diagonal elements. Given $\chi = \hat{A}_\lambda$, we have $[G_\lambda, H] = 0$, and hence all non-diagonal parts of G_λ vanish, leading to the minimization of $D(\chi)$ and achieving its global minima.

2.2.1 Dissipationless protocols

The action S can be interpreted physically as indicative of the transition rate from a given energy level to all other levels under stochastic modulation of λ with a balancing term $i\hbar\chi$. Considering a hamiltonian with added white noise,

$$H_\lambda = H(\lambda) + \dot{\lambda} \chi, \quad (2.20)$$

where $\lambda = \lambda_0 + \epsilon(t)$ and $\epsilon(t)$ represents infinitesimal white noise. Expanding H_λ gives:

$$H_\lambda \approx H(\lambda_0) + \epsilon(t) \frac{\partial H}{\partial \lambda}(\lambda_0) + \dot{\epsilon} \chi. \quad (2.21)$$

Utilizing the Fermi-Golden Rule, the transition rate Γ_n from state $|n\rangle$ is:

$$\Gamma_n = \int_{-\infty}^{\infty} d\omega S_e(\omega) \sum_{m \neq n} |\langle m | (\partial_\lambda H + \frac{i}{\hbar} [\chi, H]) | n \rangle|^2 \delta(E_m - E_n - \hbar\omega), \quad (2.22)$$

$$= \kappa \int_{-\infty}^{\infty} d\omega \sum_{m \neq n} \left| \left\langle m \left| \left(\frac{\partial H}{\partial \lambda} + \frac{i}{\hbar} [\chi, H] \right) \right| n \right\rangle \right|^2 \delta(E_m - E_n - \hbar\omega) = \kappa \langle n | G_\lambda^2(\chi) | n \rangle_{\text{connected}} \quad (2.23)$$

where $S_e(\omega) = \kappa$ denotes the noise spectral density, constant for white noise. Averaging Γ_n over all states gives the average lifetime, inversely related to Eq. (131), and minimizing this rate corresponds to reducing the action S . Now when $\chi = \mathcal{A}_\lambda$

Therefore we can see that:

$$\begin{aligned}\Gamma_n(\mathcal{A}_\lambda) &= \kappa \langle n | G_\lambda^2(\mathcal{A}_\lambda) | n \rangle_{connected} = \kappa \langle n | M_\lambda^2(\mathcal{A}_\lambda) | n \rangle_{connected} \\ &= \kappa (\langle n | M_\lambda^2(\mathcal{A}_\lambda) | n \rangle - \langle n | M_\lambda(\mathcal{A}_\lambda) | n \rangle^2) = 0\end{aligned}\tag{2.24}$$

Now since M_λ is diagonal in the eigenbasis, expectation of its square is square of its expectation, meaning $\Gamma_n = 0$. This establishes the clear reason behind considering this whole business, Transitionless Drives.

Dissipationlessness:

The lifetime of eigenstates, particularly in systems with many particles, is not a directly measurable property. A more concrete measure of dissipation is the rate of increase in energy variance, often referred to as the **dissipation rate**. If the initial eigenstate persists, no dissipation occurs, and the energy variance remains constant.

Conversely, if the eigenstate changes, the dissipation rate is positive, and the energy variance grows. In large systems obeying the eigenstate thermalization hypothesis, the dissipation rate and the heating rate are correlated, with the proportionality constant being half the reciprocal of the eigenstate's temperature. According to the Fermi golden rule, the dissipation rate commencing from the eigenstate $|n\rangle$ can be derived in a similar way as (22) by considering the transition probabilities weighted with ω^2 :

$$\frac{d\sigma_E^2}{dt} = \int_{-\infty}^{\infty} d\omega S_e(\omega) \sum_{m \neq n} \omega^2 |\langle n | (\partial_\lambda H - i\omega \chi) | m \rangle|^2 \delta(E_m - E_n - \hbar\omega)\tag{2.25}$$

$$\begin{aligned}&= -\kappa \langle n | [G_\lambda(\chi), H]^2 | n \rangle_{connected} \\ \implies \left. \frac{d\sigma_E^2}{dt} \right|_{\chi=\mathcal{A}_\lambda} &= -\kappa \langle n | [G_\lambda(\mathcal{A}_\lambda), H]^2 | n \rangle_{connected} = 0\end{aligned}\tag{2.26}$$

This averaged dissipation rate over all states $|n\rangle$ reflects the action dictated by the Frobenius norm of the commutator of $G_\lambda(X)$ with the hamiltonian. Thus, the mean dissipation rate for a system under external white noise in λ and with the compensatory term from previous equation, equates to the squared error from Eq. (19) when χ is employed as an approximate solution to Eq. (2.19).

* — *

Chapter 3

Transitionless quantum drives

An application of adiabatic gauge potentials, known as counter-diabatic driving, offers a novel approach to achieving adiabatic dynamics rapidly. This has many names, as mentioned, in the literature but following Polkovnikov et al.'s work [1] we will use the terminology, counter-diabatic drive throughout here. This technique, originating from the concept of adiabatic gauge potentials, bypasses the need for slow evolution by introducing an additional term to the hamiltonian:

Previously we identified what was causing the transition, apart from the diagonal part, which doesn't cost any transition between energy levels. Now if we evolve the system according to the hamiltonian which do not contain the terms causing transitions, we can follow the instantaneous eigenstates of the original time dependent hamiltonian.

$$\tilde{\mathcal{H}}_m(t) \rightarrow \tilde{\mathcal{H}}_m(t) + \dot{\lambda} \tilde{\mathcal{A}}_\lambda(t). \quad (3.1)$$

Moving to the original frame, we obtain an effective hamiltonian:

$$\mathcal{H}_{\text{CD}} = \mathcal{H} + \dot{\lambda} \mathcal{A}_\lambda \quad (3.2)$$

Here $\dot{\lambda} \mathcal{A}_\lambda$ represents the counter-diabatic term which ensures that the system, evolved under \mathcal{H}_{CD} will instantaneously follow the instantaneous eigenstates of the Original hamiltonian as from (3) and (5) we can see:

$$\tilde{\mathcal{H}}_{\text{CD}}(t) = U_\lambda^\dagger H_0 U_\lambda \quad (3.3)$$

And clearly, the states evolved with respect to a diagonal¹ hamiltonian $U_\lambda^\dagger H_0 U_\lambda$ will inevitably follow the immediate eigenstates at each timestamp. Therefore, the essential idea here is that - it has been possible to develop an analytically-guided protocol, such that - **When the system is driven by this counter-diabatic hamiltonian, the eigenspectrum has no transitions between energy levels.**

Therefore, if we can determine the gauge potential, maybe even by the variational approach when the exact solution is intractable (due to unsolvability) or impractical (due to computational complexity), we can develop hamiltonians like $\tilde{\mathcal{H}}_{\text{CD}}(t)$ which transitionlessly drive a system. Therefore the assignment of parameters within $\tilde{\mathcal{H}}_{\text{CD}}(t)$ are named as **protocols**, such that once the parameters are varied according to the operational form in the counter-diabatic hamiltonian $\tilde{\mathcal{H}}_{\text{CD}}(t)$, the eigenspectrum of the system do not mix as long as the original and counterdiabatic hamiltonian agree in the initial point. This is transitionlessly driving a quantum system, as approached in [1] and [2].

Note that, various authors in the condensed matter theory and quantum information theory have approached this idea from different directions, but the way Polkovnikov et al [1] has presented the idea, is more general than many explicit choices made by various authors about the nature of the unitary operator U_λ that diagonalizes the instantaneous eigenspectrum of the hamiltonian. In the following, one concrete calculation will be presented regarding Transitionless Quantum Driving as studied by

¹by construction

Berry in [2]. The extension of the idea and finding the exact parallel between the one presented by [1] remains to be explored, although it is clear that Berry makes a specific choice of the unitary operator satisfying (1).

3.1 Counter-diabatic hamiltonian

This section discusses the essential works done in [2] regarding transitionlessly driving an arbitrary single-spin under external field, providing an exact solution of a magnetic field corresponding to standard Landau-Majorana-Zener Problem of 2-level system, and adiabatic transition therein. That magnetic field will drive the instantaneous eigenstates of the LMZ hamiltonian, making sure there is not even any exponential small probability of finding the system (in fact 0), in a state in far future, not in a state it started as, in the far past.

A varying hamiltonian $\hat{H}_0(t)$ typically leads to transitions between quantum states under its influence. For gradual modifications, it is apt to utilize the adiabatic basis, the instantaneous eigenstates of $\hat{H}_0(t)$. When these changes are characterized by a small parameter ϵ , the well-known adiabatic theorem ensures that a system initially in an instantaneous eigenstate will predominantly adhere to this state as $\epsilon \rightarrow 0$. However, transitions are not entirely eliminated; traditional analyses suggest transition amplitudes are on the order of $\exp(-\text{constant}/\epsilon)$. The prototypical example is the Landau-Majorana-Zener model for two-level systems. Yet, from a 'reverse engineering' standpoint, it is feasible to construct hamiltonians $\hat{H}(t)$, corresponding to any given $\hat{H}_0(t)$, that precisely drive the instantaneous eigenstates of $\hat{H}_0(t)$ without transitions, regardless of the magnitude of ϵ . A general expression for such $\hat{H}(t)$ is provided. This includes scenarios like spins in varying magnetic fields, suggesting the existence of classical spin trajectories unaltered by such fields. For spin 1/2, this concept is akin to the two-state quantum dynamics, where the LMZ model is adjusted to a variant without transitions.

Berry develops the algorithm for counter-diabatic drive in a unique way, for small change in parameter value, i.e. assuming adiabaticity conditions to hold. It is known that given the instantaneous eigenstates

$$\hat{H}_0(t) |n_t\rangle = E_n(t) |n_t\rangle \quad (3.4)$$

and considering only leading contribution from the parameter change (i.e. assuming adiabaticity):

$$|\psi_n(t)\rangle = \exp \left\{ -\frac{i}{\hbar} \int_0^{t'} d\tau E_n(\tau) - \int_0^{t'} d\tau \langle n_\tau | \partial_\tau n_\tau(\tau) \rangle \right\} |n(t)\rangle \quad (3.5)$$

Are the states evolving dynamically under the time-evolution of the hamiltonian $\hat{H}_0(t)$ including the effect of leading contributions from the adiabatic correction corresponding the change of parameters in that hamiltonian.

Now if we wish to determine the hamiltonian that causes the Exact Time Evolution of these $|\psi_n(t)\rangle$, i.e. the hamiltonian, for which $|\psi_n(t)\rangle$ solves the Schrodinger Equation. The problem can be posed by a slightly different way.

Fix a basis, say the Hamilton for **any fixed time t' when the effect of the time-dependence is 0**. With Landau-Zener-Majorana problem in mind, with linear separation of eigenenergies of a 2 level system, that time is $t' = 0$ (i.e. with vt as the ramp, the hamiltonian becomes independent of the time-dependent-coupling-parameter, only at $t = 0$), so that parameter dependence vanishes at $t = 0 = t'$. Now determine its eigenspectrum say $\{|n_0\rangle\}$, therefore with knowing dynamically evolving states for small changes:

$$|\psi_{n, \lambda}(t)\rangle = \exp \left(-\frac{i}{\hbar} \int_0^t E_n(\lambda) d\lambda + \frac{i}{\hbar} \int_0^t \mathcal{A}_t^{(n)} dt \right) |n_t\rangle, \quad \text{with,} \quad \mathcal{A}_t^{(n)} = i\hbar \langle n_t | \partial_t n_t \rangle, \quad \text{where}$$

For berry, that comoving frame was the $|n_0\rangle$, and the unitary transformation is the

$$U(t) = \exp \left(-\frac{i}{\hbar} \int_0^t E_n(\lambda) d\lambda + \frac{i}{\hbar} \int_0^t \mathcal{A}_t^{(n)} dt \right) |n_t\rangle \langle n_0| \implies 0 = \partial_\lambda(|n_0\rangle) = \partial_\lambda(U^\dagger |\psi_\lambda(t)\rangle) \quad (3.6)$$

And we want the hamiltonian, that generates this time unitary transformation. So that we can have :

$$i\hbar \partial_t U(t) = H(t)U(t) \implies H(t) = i\hbar(\partial_t U(t)) U^\dagger \quad (3.7)$$

Once calculated, this gives an explicit form of a hamiltonian that exactly evolves the instantaneous eigenspectrum of the original time-dependent hamiltonian $H_0(t)$ without any transitions in the dynamics, although with arbitray time-dependence in the problem. Berry calls this idea **Reverse-Engineering**, so that:

$$\hat{H}(t) = \sum_n |n\rangle E_n \langle n| + i\hbar \sum_n |\dot{n}\rangle \langle n| - \langle n|\dot{n}\rangle |n\rangle \langle n| = \hat{H}_0(t) + \hat{H}_1(t) \quad (3.8)$$

The additional term can be simplified further by using that

$$\langle m|\partial_t n\rangle = \frac{\langle m|\partial_t \hat{H}_0|n\rangle}{E_n - E_m} \implies \hat{H}_1(t) = i\hbar \sum_{m \neq n} \frac{|m\rangle \langle m|\partial_t \hat{H}_0|n\rangle \langle n|}{E_n - E_m} \quad (3.9)$$

Now that we don't have any $|\partial_t n\rangle$ involved in the problem, and we can do every calculation once the instantaneous eigenspectrum $\{|n_t\rangle\}$ has been obtained.

3.1.1 Transitionless evolution of classical spin trajectories

For a particle with spin in a time-dependent magnetic field $B_0(t)$, the hamiltonian $\hat{H}_0(t)$ is defined by the interaction with the spin vector \vec{S} , as follows:

$$\hat{H}_0(t) = \gamma \mathbf{B}_0(t) \cdot \vec{S}, \quad (3.10)$$

where γ denotes the gyromagnetic ratio and \vec{S} represents the spin operator for a particle with any spin quantum number s . For spin-half particles

$$\vec{S} = \frac{\hbar}{2} \{\sigma_x, \sigma_y, \sigma_z\}, \quad (3.11)$$

in terms of the Pauli matrices. For a general spin state,

$$\hat{H}_1(t) = i\hbar\gamma \partial_t \mathbf{B}_0 \cdot \sum_{m \neq n} \frac{|m\rangle \langle m|\vec{S}|n\rangle \langle n|}{E_n - E_m}, \quad (3.12)$$

which is an expression for the time-dependent perturbation in the hamiltonian due to the magnetic field. The eigenvalues are given by $E_n = \gamma\hbar n B_0(t)$. Now going to the coordinate where the $\hat{n}z$ and $B_0(t)$ are aligned exactly, and using the standard expressions -

$$\langle n|S_z|n\rangle = \hbar n, \quad \langle n \pm 1|S_x|n\rangle = \frac{1}{2}\hbar\sqrt{s(s+1) - n(n \pm 1)}, \quad \& \quad \langle n \pm 1|S_y|n\rangle = \mp \frac{i}{2}\hbar\sqrt{s(s+1) - n(n \pm 1)} \quad (3.13)$$

we can obtain

$$\hat{H}_1 = \frac{1}{B_0} (\partial_t B_{0x} \hat{S}_y - \partial_t B_{0y} \hat{S}_x), \quad (3.14)$$

And reverting to the original basis we find:

$$\hat{H}_1 = \frac{1}{B_0^2} \partial_t \mathbf{B}_0 \times \vec{S} \cdot \mathbf{B}_0 = \frac{1}{B_0^2} \mathbf{B}_0 \times \partial_t \mathbf{B}_0 \cdot \vec{S} = \mathbf{b}_0 \times \partial_t \mathbf{b}_0 \cdot \vec{S} \quad \text{with} \quad \mathbf{b}_0 = \frac{\mathbf{B}_0}{B_0} \quad (3.15)$$

with this our resultant hamiltonian becomes:

$$\hat{H}(t) = \gamma \left[\mathbf{B}_0(t) + \frac{1}{B_0(t)^2} \mathbf{B}_0(t) \times \partial_t \mathbf{B}_0(t) \right] \cdot \hat{\mathbf{S}} = \gamma \left[\mathbf{B}_0(t) + \frac{1}{\gamma} b_0(t) \times \partial_t b_0(t) \right] \cdot \hat{\mathbf{S}} = \gamma \mathbf{B}(t) \cdot \hat{\mathbf{S}} \quad (3.16)$$

Since the original system is driven by the magnetic field $\mathbf{B}_0(t)$ the extreme eigenstates (all the eigenstates of a 2-level or spin- $\frac{1}{2}$ problem)

$$\mathbf{S} \equiv \langle \psi_n(t) | \hat{\mathbf{S}} | \psi_n(t) \rangle \implies \mathbf{S}(t) = \pm b_0(t) \quad (3.17)$$

$$\implies \mathbf{B}(t) = B_0(t) \mathbf{S}(t) + \frac{1}{\gamma} \mathbf{S}(t) \times \partial_t \mathbf{S}(t) \quad (3.18)$$

This is the Magnetic Field of a hamiltonian defined as (36) that exactly evolves the instantaneous eigenstates of the original hamiltonian $H_0(t)$ without dissipation or transition, in its full generality.

3.2 A transitionless LZM problem

In the classic Landau–Zener–Majorana two-level model, the driving field follows a linear trajectory in B space, advancing at a constant velocity V with the closest approach B_{\min} to the zero-field point. To achieve transitionless evolution (without spin precession), $B_0(t)$ is chosen as:

$$B_0(t) = B_{\min} e_x + V t e_z. \quad (3.19)$$

The spin vector evolves as:

$$\mathbf{S}(t) = \frac{B_{\min} e_x + V t e_z}{\sqrt{B_{\min}^2 + V^2 t^2}}, \quad (3.20)$$

describing a great circle trajectory on the Bloch sphere, from south to north pole as t goes from negative to positive infinity.

The magnetic field driving this spin transitionless trajectory is given by:

$$\mathbf{B}(t) = B_{\min} e_x + V t e_z - \frac{e B_{\min} V}{B_{\min}^2 + V^2 t^2} e_y, \quad (3.21)$$

which ensures the desired spin evolution.

This *reverse engineering* approach seeks to determine which hamiltonian $\hat{H}(t)$ will generate a desired evolution, i.e., states that are instantaneous eigenstates of a given hamiltonian $\hat{H}_0(t)$. The reverse-reverse engineering perspective, originally proposed by Berry in [2], inverts this problem: it identifies the instantaneous eigenspectrum by a specified hamiltonian $\hat{H}(t)$, which entails solving for $\hat{H}_0(t)$ using the time-dependent Schrödinger equation.

3.2.1 A reverse-reverse engineering perspective

Now that we know, given a hamiltonian how to obtain the hamiltonian that evolves the system without (in principle) causing any transition, we wish to know, given the complete solution of the time-dependent Schrodinger Equation, what is the hamiltonian whose instantenous eigenvalues are this, meaning that we wish to find the comoving-frame of the time-dependent system.

For that, and for brevity now consider $\mathbf{B}(t) = 2\{1, 0, t\}$ where $V = 2 = B_{\min}$ has been assumed:

$$i\hbar \partial_t |\psi(t)\rangle = i\hbar \partial_t \begin{pmatrix} u(t) \\ v(t) \end{pmatrix} = \gamma \begin{pmatrix} t & 1 \\ 1 & -t \end{pmatrix} \begin{pmatrix} u(t) \\ v(t) \end{pmatrix} \quad (3.22)$$

Which gives

$$(i\partial_t - \gamma t)u(t) = \gamma v(t) \quad \& \quad (i\partial_t + \gamma t)v(t) = \gamma u(t) \quad (3.23)$$

decoupling them, and making the transformation $t \rightarrow z = t\sqrt{2\gamma}e^{\frac{3\pi i}{4}}$ we obtain:

$$\partial_z c_i(z) = (\nu_i + \frac{1}{2} - \frac{z^2}{2})c_i(z) = 0 \quad (3.24)$$

$$\text{where, } c_1(z) = u(z), c_2(z) = v(z), \quad \& \quad \nu_1 = \frac{i\gamma}{2} - 1, \quad \nu_2 = \frac{i\gamma}{2} \quad (3.25)$$

Which is the known **Weber Equation**, whose solutions are **Weber Functions** or **Parabolic Cylinder Functions**, and there are 2 orthogonal solutions to every such equations. So the differential equation of the kind above, has the following general solution :

$$\frac{\partial^2 y(z)}{\partial z^2} + (\mu + \frac{1}{2} - \frac{z^2}{4})y(z) = 0, \quad (3.26)$$

$$\text{has 2 orthogonal solutions: } y = D_\mu(z), \quad \& \quad y = D_{-\mu-1}(iz)$$

Therefore General Solution for the components of the wavefunction are the following:

$$u(t) = U_1 D_{i\frac{\gamma}{2}-1}(t\sqrt{2\gamma} e^{\frac{3\pi i}{4}}) + U_2 D_{-i\frac{\gamma}{2}}(t\sqrt{2\gamma} e^{\frac{3\pi i}{4}}), \quad \& \quad (3.27)$$

$$v(t) = V_1 D_{i\frac{\gamma}{2}}(t\sqrt{2\gamma} e^{\frac{3\pi i}{4}}) + V_2 D_{-i\frac{\gamma}{2}-1}(t\sqrt{2\gamma} e^{\frac{3\pi i}{4}})$$

Now we demand the Physical Conditions, which are

$$u(t \rightarrow -\infty) = 0 \quad \& \quad |v(t \rightarrow -\infty)| = 1 \quad (3.28)$$

Meaning that the state started with $\begin{pmatrix} 0 \\ 1 \end{pmatrix}$ in the past infinity. Now looking at $v(t)$ first, we note the asymptotics, as $t \rightarrow -\infty$

$$D_{-i\frac{\gamma}{2}-1}(t\sqrt{2\gamma} e^{\frac{3\pi i}{4}}) \rightarrow -i2^{-i\frac{\gamma}{2}-1}\gamma t^2 e^{-i\frac{\gamma}{2}t^2} \sinh(\frac{\pi\gamma}{8}) \rightarrow \infty + \text{High Oscillations} \quad (3.29)$$

Thus, this do not contribute in the expression of $v(t)$ and for the other component we must have, as $t \rightarrow -\infty$:

$$v(t \rightarrow -\infty) \rightarrow V_1 \left(2^{\frac{i\gamma}{4}} e^{i\frac{\gamma}{2}t^2} (i\gamma t^2)^{\frac{i\gamma}{4}} \{ \cosh(\frac{\pi\gamma}{8}) + \sinh(\frac{\pi\gamma}{8}) \} \right), \quad \text{thus} \quad (3.30)$$

$$|v(t \rightarrow -\infty)| = 1 \implies V_1^2 (\cosh(\frac{\pi\gamma}{8}) + \sinh(\frac{\pi\gamma}{8}))^{-2} \implies V_1 = e^{-\frac{\pi\gamma}{8}} \quad (3.31)$$

Therefore we got

$$v(t) = e^{-\frac{\pi\gamma}{8}} D_{i\frac{\gamma}{2}}(t\sqrt{2\gamma} e^{\frac{3\pi i}{4}}) \quad (3.32)$$

, Now putting this back into the second part of (49), and using the following identity:

$$D'_\nu(z) + \frac{1}{2}zD_\nu(z) - \nu D_{\nu-1}(z) = 0 \quad (3.33)$$

and noting that

$$D_{-i\frac{\gamma}{2}}(t\sqrt{2\gamma} e^{\frac{3\pi i}{4}}) \rightarrow (-i\gamma t^2)^{i\frac{\gamma}{4}} 2^{-i\frac{\gamma}{4}} e^{-i\frac{\gamma}{2}t^2} \frac{\sqrt{\gamma} \cosh(\frac{\pi\gamma}{8})}{\Gamma(\frac{i\Gamma}{2})} \neq 0 \quad (3.34)$$

This gives us:

$$u(t) = U_1 D_{i\frac{\gamma}{2}-1}(t\sqrt{2\gamma} e^{\frac{3\pi i}{4}}) \quad (3.35)$$

$$\text{which gives us: } U_1 = i\sqrt{\frac{i\gamma}{2}} e^{-\frac{\pi\gamma}{8}} \quad (3.36)$$

Thus putting them all together we get that:

$$\begin{pmatrix} u(t) \\ v(t) \end{pmatrix} = e^{-\frac{\pi\gamma}{8}} \begin{pmatrix} i\sqrt{\frac{i\gamma}{2}} D_{i\frac{\gamma}{2}-1}(t\sqrt{2\gamma} e^{\frac{3\pi i}{4}}) \\ D_{i\frac{\gamma}{2}}(t\sqrt{2\gamma} e^{\frac{3\pi i}{4}}) \end{pmatrix} \quad (3.37)$$

And this satisfies $|u|^2 + |v|^2 = 1$ Now that we have exact time-dependent evolving state of the Landau-Zener-Majorana hamiltonian, we wish to know, given what kind of magnetic field, these are the instantaneous eigenstates. This can be done by reversing the previously developed argument about transitionless drive.

The corresponding evolving spin is given exactly by (43) as

$$\mathbf{S}(t) = \{2\text{Re}[u^* v], 2\text{Im}[u^* v], |u|^2 - |v|^2\} \quad (3.38)$$

From this exact solution, we wish to find the $B_0(t)$ from (44) by

$$\mathbf{B}_0(t) = (\mathbf{B}(t) \cdot \mathbf{S}(t)) \mathbf{S}(t) = 2[2\text{Re}[u^* v] + t(|u|^2 - |v|^2)] \mathbf{S}(t) \quad (3.39)$$

Which can be plotted for $\gamma = 2.5$ and $\gamma = 1$ as:

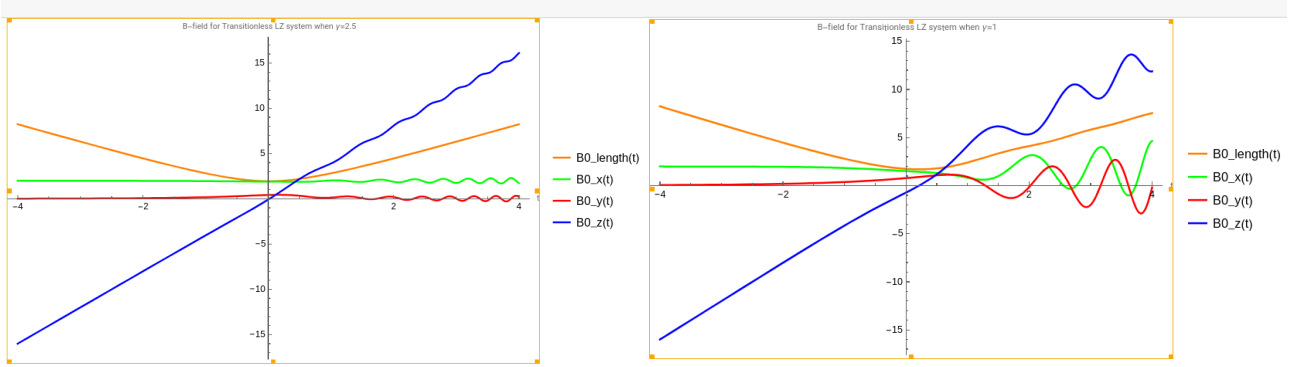


Figure 3.1: Transitionless driving field for $\gamma = 2.5$ Figure 3.2: Transitionless driving field for $\gamma = 1$

This is the magnetic field $B_0(t)$ for Landau–Majorana–Zener hamiltonian whose eigenstates are exact time-dependent states for driving field $B(t) = 2\{1, 0, t\}$.

* — *

Chapter 4

AGP for many-body systems

4.1 XY Spin- $\frac{1}{2}$ chain with transverse magnetic field (XYTF)

As discussed in [1], minimization of the action (17) can be used to determine AGP in complex quantum systems, and if these are integrable theories, then an exact form can be obtained using the known solution of the theory, restricted to some fixed state.

The model is given as:

$$\mathcal{H} = - \sum_{j=1}^L \left(J_x \sigma_j^x \sigma_{j+1}^x + J_y \sigma_j^y \sigma_{j+1}^y + h \sigma_j^z \right) \quad (4.1)$$

with : $J_x = J \left(\frac{1+\gamma}{2} \right), \quad J_y = J \left(\frac{1-\gamma}{2} \right)$

Now this can be mapped into a free-fermion theory, so that it gives a plethora of analytical properties of AGPs that can be studied extensively. Now there is an additional tuning parameter that needs to be considered, which is rotating all the spins about the z -axis by an angle of $\frac{\phi}{2}$, because - even though the spectrum does depend on this parameter, the ground states do [1] [3]:

To rotate the spins around the z -axis by an angle $\frac{\phi}{2}$, we use the rotation operator: $R_z \left(\frac{\phi}{2} \right) = e^{-i \frac{\phi}{4} \sigma_z}$ so that the spin degrees of freedom transform as:

$$\begin{aligned} \begin{pmatrix} \sigma_j^x & \sigma_j^y & \sigma_j^z \end{pmatrix} &\rightarrow \begin{pmatrix} \sigma_j^x & \sigma_j^y & \sigma_j^z \end{pmatrix} \begin{pmatrix} \cos\left(\frac{\phi}{2}\right) & \sin\left(\frac{\phi}{2}\right) & 0 \\ -\sin\left(\frac{\phi}{2}\right) & \cos\left(\frac{\phi}{2}\right) & 0 \\ 0 & 0 & 1 \end{pmatrix} \\ &= \left(\cos\left(\frac{\phi}{2}\right) \sigma_j^x + \sin\left(\frac{\phi}{2}\right) \sigma_j^y, \cos\left(\frac{\phi}{2}\right) \sigma_j^y - \sin\left(\frac{\phi}{2}\right) \sigma_j^x, \sigma_j^z \right) \end{aligned}$$

Consider $J = 1$ setting the energy scale we find:

$$\mathcal{H} \rightarrow - \sum_{j=1}^L \left\{ \frac{\gamma}{2} \cos(\phi) \left[\sigma_j^x \sigma_{j+1}^x - \sigma_j^y \sigma_{j+1}^y \right] + \frac{\gamma}{2} \sin(\phi) \left(\sigma_j^y \sigma_{j+1}^x + \sigma_j^x \sigma_{j+1}^y \right) + \frac{1}{2} \left[\sigma_j^x \sigma_{j+1}^x + \sigma_j^y \sigma_{j+1}^y \right] + h \sigma_j^z \right\}$$

Now, After Jordan-Wigner transformation, and then considering the Nambu-Spinors as: $\psi_k^\dagger = (c_k^\dagger, c_{-k})$ i.e. by using:

$$\text{using : } c_j^\dagger = \left(\prod_{n < j} \sigma_n^z \right) \sigma_j^-, \quad c_j = \left(\prod_{n < j} \sigma_n^z \right) \sigma_j^+, \quad \& \quad \sigma_i^z = (1 - 2c_i^\dagger c_i) \quad (4.2)$$

$$\text{and going to the momentum space using : } c_k = \frac{1}{\sqrt{M}} \sum_j c_j e^{-ikr_j}$$

$$\text{we obtain: } \mathcal{H} = \sum_k \psi_k^\dagger H_k \psi_k, \quad H_k = \begin{pmatrix} h - \cos(k) & \gamma \sin(k) e^{i\phi} \\ \gamma \sin(k) e^{-i\phi} & -h + \cos(k) \end{pmatrix} \quad (4.3)$$

4.1.1 Derivation using the variational principle

To derive the precise gauge potential, it is essential to ascertain the potential for a series of disentangled two-level systems governed by H_k . While various established techniques are applicable, adopting the minimal action strategy is prudent in this context, especially for subsequent juxtaposition with variational estimates. Thus, we employ this principle to systematically develop the equation for each parameter: h , γ , and ϕ . Therefore in this form, we can choose an Ansatz for the AGP, and try to optimize the parameters of it. So consider:

$$A(k) = \frac{1}{2} (\alpha_x(k)\sigma_k^x + \alpha_y(k)\sigma_k^y + \alpha_z(k)\sigma_k^z) \quad (4.4)$$

so that the commutator with the hamiltonian becomes:

$$\begin{aligned} i[A(k), H_k] &= [\alpha_y(h - \cos k) - \alpha_z\gamma \sin k \sin \phi] \sigma_k^x + [\alpha_z\gamma \sin k \cos \phi - (h - \cos k)\alpha_x] \sigma_k^y \\ &\quad + \gamma \sin k [\alpha_x \sin \phi - \alpha_y \cos \phi] \sigma_k^z \end{aligned} \quad (4.5)$$

Therefore we get, considering a time dependent $h(t)$ for the problem:

$$S_h = \text{Tr}[G_\lambda^2] \quad (4.6)$$

$$\begin{aligned} &= \text{Tr}[(\partial_h \mathcal{H}_k + i[A(k), H_k])^2] = 2 \left[[-1 + \alpha_x\gamma \sin k \sin \phi - \alpha_y\gamma \sin k \cos \phi]^2 \right. \\ &\quad \left. + [\alpha_y(h - \cos k) - \alpha_z\gamma \sin k \sin \phi]^2 + [\alpha_z\gamma \sin k \cos \phi - (h - \cos k)\alpha_x]^2 \right] \end{aligned} \quad (4.7)$$

Minimizing this gives us the AGP:

$$A_h = \frac{1}{2} \sum_k \frac{\gamma \sin k}{(\cos k - h^2) + \gamma^2 \sin^2 k} \psi_k^\dagger (\sin \phi \sigma_k^x - \cos \phi \sigma_k^y) \psi_k \quad (4.8)$$

In order to facilitate an analytical discussion of the real space representation, we confine our parameters to the transverse field Ising model limit, where $\gamma = 1$ and $\phi = 0$. It is important to first note that, by applying a Fourier transform, we obtain

$$\mathcal{A}_h = \sum_{l=1}^M \alpha_l \mathcal{O}_l, \quad \text{with} \quad \alpha_l = -\frac{1}{4L} \sum_k \frac{\sin(k) \sin(lk)}{(\cos k - h)^2 + \sin^2 k}, \quad \mathcal{O}_l = 2i \sum_j (c_j^\dagger c_{j+l}^\dagger - c_{j+l} c_j) \quad (4.9)$$

The behaviour of the function α_l we can make a plot of the kind here:

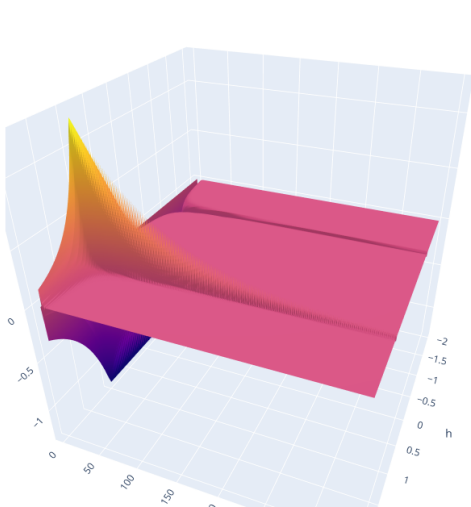


Figure 4.1: $\alpha_l(h)$: point of view - A

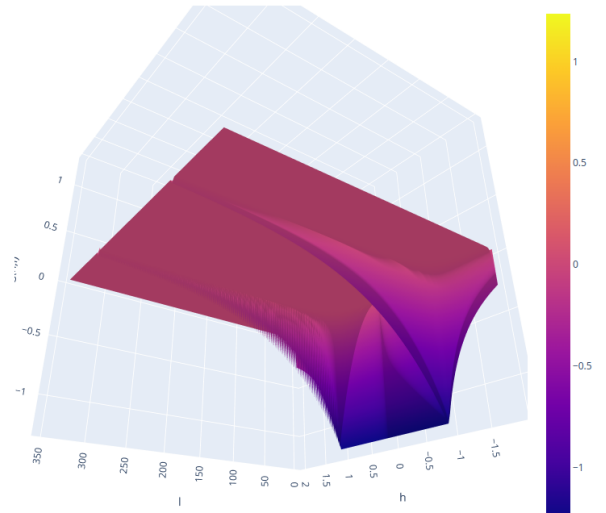


Figure 4.2: $\alpha_l(h)$: point of view - $A_{\text{antipodal}}$

So that we can clearly see the effect of highly nonlocal overlap between distant sites operations near the critical point, which require further investigation.

4.2 AGP for the ground state

With the Bloch hamiltonian (4.3) at hand we can do further investigation of the Ground State of the quantum XY spin chain with transverse magnetic field and find out how it changes under change of the parameter in the systems, and determine qualitative changes of the Ground State, to identify and analyse the Phases and Phase Transitions using the formalism of adiabatic gauge potential. For that, notice for general hamiltonian of the following kind, we can obtain the lowest energy eigenstate and determine how it changes under varying parameters. So consider $A = -(h - \cos k)$ & $B = -\gamma \sin k$

$$\begin{aligned} \mathcal{H}_k &= \begin{pmatrix} A & Be^{i\phi} \\ Be^{-i\phi} & -A \end{pmatrix} \rightarrow \begin{pmatrix} A - \lambda_- & Be^{i\phi} & | 0 \rangle \\ Be^{-i\phi} & -(A + \lambda_-) & | 0 \rangle \end{pmatrix} \rightarrow \begin{pmatrix} (A - \lambda_-) & Be^{i\phi} & | 0 \rangle \\ 0 & 0 & | 0 \rangle \end{pmatrix} \\ &\Rightarrow |gs_k\rangle = x \begin{pmatrix} e^{i\frac{\phi}{2}} \\ \frac{(\lambda_- - A)}{B} e^{-i\frac{\phi}{2}} \end{pmatrix} \end{aligned} \quad (4.10)$$

Where x can be thought of as a Normalizing Factor that we need not to worry about as that doesn't contain any information of the state's dependence on the parameters of the theory. Moreover representing our state in the Qubit language in the Bloch Sphere (where for each momentum mode, we should think of the system as independent Qubits), we have for our Ground State -

$$\begin{pmatrix} 1 \\ 0 \end{pmatrix} \equiv |0\rangle_k \text{ \& } \begin{pmatrix} 0 \\ 1 \end{pmatrix} \equiv |1\rangle_k \text{ gives } |gs\rangle_k = \cos \frac{\theta_k}{2} e^{i\frac{\phi}{2}} |0\rangle_k + \sin \frac{\theta_k}{2} e^{-i\frac{\phi}{2}} |1\rangle_k \quad (4.11)$$

$$\text{therefore: } \tan \frac{\theta_k}{2} = \frac{(\lambda_- - A)}{B} \Rightarrow \theta_k = \tan^{-1} \left(\frac{\gamma \sin k}{h - \cos k} \right) \quad (4.12)$$

This is the polar angle of the ground state represented in the Bloch Sphere, and it incorporates all the information that we need about parameter-dependence of the Ground State of this system, and will turn out very important as we will demonstrate in the following sections. Now look at how this state varies under varying parameters:

$$\partial_h |gs\rangle_k = \frac{\partial_h \theta_k}{2} \begin{pmatrix} -\sin \frac{\theta_k}{2} e^{i\frac{\phi}{2}} \\ \cos \frac{\theta_k}{2} e^{-i\frac{\phi}{2}} \end{pmatrix} = \frac{\partial_h \theta_k}{2} \partial_h |es\rangle_k \quad (4.13)$$

Which is just the same γ and h , so that we can generalize this. So [with $\{\lambda\} \equiv \{h, \gamma\}$] and $\tau_k^{x,y,z}$; which are Pauli Matrices acting on the Instantaneous Ground/Excited States in the Bloch Sphere i.e. $\tau_k^z |gs\rangle_k = |gs\rangle_k$ & $\tau_k^z |es\rangle_k = -|es\rangle_k$ - we find the Gauge Potentials to be:

$$\mathcal{A}_\lambda = \frac{1}{2} \sum_k (\partial_\lambda \theta_k) \tau_k^y \quad \& \quad \mathcal{A}_\phi = \frac{1}{2} \sum_k [\cos(\theta_k) \tau_k^z + \sin(\theta_k) \tau_k^x - 1] \quad (4.14)$$

Note further that (4.8) and (4.14) are exactly same after identifying $\psi_k^\dagger (\sin \phi \sigma_k^x - \cos \phi \sigma_k^y) \psi_k \equiv \tau_k^y$ which is just Pauli Matrices for a rotated basis. It is that basis in which the hamiltonian takes the form of

$$H_k = -\sqrt{(h - \cos k)^2 + \gamma^2 \sin^2 k} \tau_k^z$$

* - *

Chapter 5

A geometric perspective of quantum information

Understanding the Collection of Ground States and their overall dependencies on the parameters in a theory is crucial in modern physics, especially in studying the Nature of Phases and Phase-Transitions in Many-Body Quantum Systems. A common approach involves characterizing different phases using *invariant* quantities like the Chern Number, which measures the integral of Berry curvature over a parameter space. Examples of such phases include the quantum Hall effect, topological insulators, and various spin chains. When Berry curvature is non-zero, it often indicates a break in time-reversal symmetry, either explicitly through external factors or implicitly by dividing the ground state collection into distinct sectors, each with its own broken symmetry where the degeneracies in the system, or the gap-closing points may act as monopolar sources of this disguised magnetic field.

Apart from Berry curvature, another important aspect is the Quantum Metric Tensor, which is a glorified susceptibility, something that measures the overlaps between the Bloch States as slight changes in the parameters are made. This metric is essential for understanding the properties of many-body systems and is crucial in modern day research in Quantum Information Theory. For instance, the diagonal elements of this tensor are fidelity susceptibilities, which are one of the most significant quantities in studying quantum phase transitions, including topological ones.

This report aims to investigate the Quantum Geometry of an Integrable model, the Quantum Spin-1/2 XY chain in a Transverse Field. By analyzing the geometry and Topology of the Ground State Manifold as a function of three parameters Transverse Magnetic Field (h), Interaction Anisotropy (γ), and Global Spin Rotation (ϕ), we uncover insights using techniques from Riemann geometry. By examining two-dimensional cuts of the three-dimensional metric, we reveal the shapes of different phases, Curvature Scalar, Geometric Invariants, etc and show their resilience against perturbations. We also classify singularities that occur along certain cuts, identifying three types: Integrable, Conical, and Curvature Singularities. Finally, we discuss the circumstances under which each type of singularity arises.

We now explore the geometric properties of the rich phase diagram of a quantum XY spin $\frac{1}{2}$ chain with transverse magnetic field.

5.1 Fidelity susceptibility

We start by recalling the known understanding about the Zero-Temperature phases in this model from Fig. ???. There is a -

- Phase Transition between *paramagnetic* and *Ising ferromagnetic* at $|h| = 1$ & $\gamma \neq 0$,
- Critical Line at the *Isotropy Point* at $\gamma = 0$ when $|h| < 1$,

- Meeting of two transitions at *Multi-Critical Points* when $\gamma = 0, |h| = 1$,
- Pair of special lines $|h| > 1$ & $\gamma = 0$ where the Ground State is fully polarized along the applied magnetic field and thus independent of the magnetic field. These lines have vanishing susceptibilities including vanishing metric along h -direction, and
- Line Corresponding to Transverse Field Ising Chain when $\gamma = 1$.

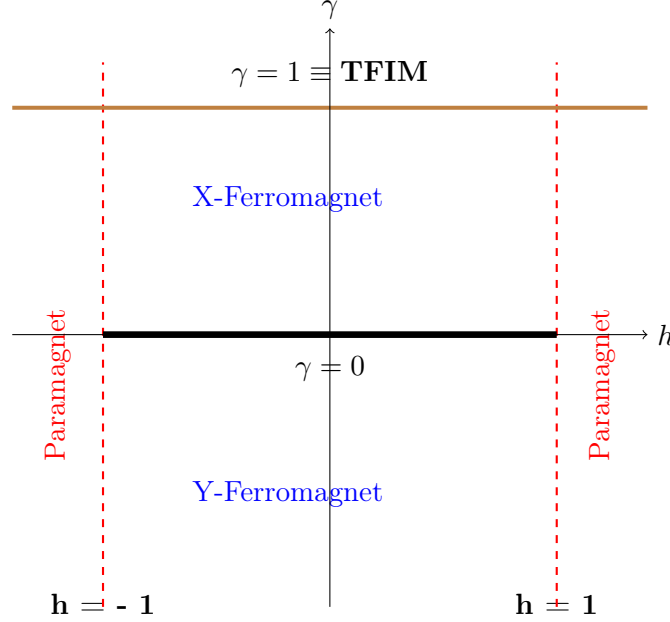


Figure 5.1: Phase Diagram of Quantum XY Chain with Anisotropy (γ) and under Transverse Magnetic Field (h)

The purpose of this section is to provide a Riemannian Geometric perspective of the Phases and the Universal Nature of the Transitions. So we start by introducing how a smooth metric captures the response of a Quantum Many-Body System in the sense that its Diagonal Elements are Fidelity Susceptibilities [1] [5]

Riemannian Geometric characterisation of distances between Ground States of Quantum Systems in the parameter space were first introduced by Provost and Vallee in 1980 [4]. Formally the geometric tensor can be defined for any manifold of states smoothly varying with some parameter $\vec{\lambda} \mapsto |\psi(\vec{\lambda})\rangle$, but for our analysis we will restrict ourselves with only the Collection of Ground States and see study their dependencies with the parameters. This geometric tensor naturally arises when one defines the distance ds between nearby states $|\psi_0(\vec{\lambda})\rangle$ and $|\psi_0(\vec{\lambda} + \delta\vec{\lambda})\rangle$ such that:

$$ds^2 \equiv 1 - \mathcal{F}(\vec{\lambda}, \vec{\lambda} + \delta\vec{\lambda})^2 = 1 - |\langle\psi_0(\vec{\lambda})|\psi_0(\vec{\lambda} + \delta\vec{\lambda})\rangle|^2 = \delta\lambda^\alpha \chi_{\alpha\beta} \delta\lambda^\beta + \mathcal{O}(\delta\vec{\lambda}^3) \quad (5.1)$$

Where $\chi_{\alpha\beta}$ is known as the Geometric Tensor and $\mathcal{F}(\vec{\lambda}_1, \vec{\lambda}_2) = |\langle\psi_0(\vec{\lambda}_1)|\psi_0(\vec{\lambda}_2)\rangle|$ is called the Fidelity, or just the probability to find the ground state at the final parameter value of $\vec{\lambda}_2$ when initially started with $\vec{\lambda}_1$ maintaining time-ordering. So it measures the probability of a state to remain itself when parameters are changed and this distance or line-element (ds^2) measures the probability of a system to leave its initial state under arbitrarily little change in the parameters. A very physical derivation is presented in [1] as the following. Consider the amplitude

$$a_n = \langle\psi_0(\vec{\lambda})|\psi_0(\vec{\lambda} + \delta\vec{\lambda})\rangle \approx \delta\lambda_\alpha \langle n | \overset{\leftarrow}{\partial}_\alpha | 0 \rangle = -\delta\lambda_\alpha \langle n | \partial_\alpha | 0 \rangle \quad (5.2)$$

Where $\overset{\leftarrow}{\partial}_\lambda$ indicates that it acts on the left where without any arrow, derivatives are meant to act on its right; also to shorten the notation we use $\partial_{\lambda_\alpha} \equiv \partial_\alpha$ & $|n\rangle \equiv |\psi_n(\vec{\lambda})\rangle$. Now recall from (2.7)

$$i\langle n | \partial_\alpha | m \rangle = \langle n | \mathcal{A}_\alpha | m \rangle \implies a_n = -\delta\lambda_\alpha \langle n | \partial_\alpha | 0 \rangle = i\langle n | \mathcal{A}_\alpha | 0 \rangle \delta\lambda_\alpha \quad (5.3)$$

Therefore we see that the amplitude of a state making a transition to any excited state at leading order in $\delta\vec{\lambda}$ is proportional to the matrix element of the Gauge Potential. Now the total probability of the Ground State to excite to any other state is therefore given by:

$$ds^2 := \sum_{n \neq 0} |a_n|^2 = \sum_{n \neq 0} \delta\lambda_\alpha \delta\lambda_\beta \langle 0 | \mathcal{A}_\alpha | n \rangle \langle n | \mathcal{A}_\beta | 0 \rangle + \mathcal{O}(\delta\vec{\lambda}^3) = \delta\lambda_\alpha \delta\lambda_\beta \langle 0 | \mathcal{A}_\alpha \mathcal{A}_\beta | 0 \rangle_c + \mathcal{O}(\delta\vec{\lambda}^3) \quad (5.4)$$

Where this subscript c means that we are taking the connected correlation function (a.k.a. the Covariance) as :

$$\langle 0 | \mathcal{A}_\alpha \mathcal{A}_\beta | 0 \rangle_c \equiv \langle 0 | \mathcal{A}_\alpha \mathcal{A}_\beta | 0 \rangle - \langle 0 | \mathcal{A}_\alpha | 0 \rangle \langle 0 | \mathcal{A}_\beta | 0 \rangle \equiv \chi_{\alpha\beta} \quad (5.5)$$

This covariance determines the Geometry Tensor introduced by Provost and Vallee [4], and in terms of the many-body wavefunction of the ground state, it can be expressed as:

$$\chi_{\alpha\beta} = \langle 0 | \overleftarrow{\partial}_\alpha \partial_\beta | 0 \rangle_c = \langle \partial_\alpha \psi_0 | \partial_\beta \psi_0 \rangle_c = \langle \partial_\alpha \psi_0 | \partial_\beta \psi_0 \rangle - \langle \partial_\alpha \psi_0 | \psi_0 \rangle \langle \psi_0 | \partial_\beta \psi_0 \rangle \quad (5.6)$$

Note that the last expression here is to protect the invariance of this distance under arbitrary $U(1)$ transformation of the kind $\psi_0(\vec{\lambda}) \rightarrow e^{i\Phi(\vec{\lambda})} \psi_0(\vec{\lambda})$. But this object is not necessary always symmetric, but the Gauge Potentials are Hermitian, and one can show therefore that the Geometric Tensor is also hermitian as $\chi_{\alpha\beta}^* = \chi_{\beta\alpha}$ where only the symmetric part of $\chi_{\alpha\beta}$ determines the distance between the states; which in the quadratic form becomes:

$$g_{\alpha\beta} = \frac{1}{2}(\chi_{\alpha\beta} + \chi_{\beta\alpha}) = \frac{1}{2} \langle 0 | \{ \mathcal{A}_\alpha \mathcal{A}_\beta | 0 \} \rangle_c \quad (5.7)$$

Which is more familiar to the Quantum Information Community as Fubini-Study Metric of the Ground State Manifold. The antisymmetric part of the geometric tensor defines the Berry Curvature through

$$F_{\alpha\beta} = i(\chi_{\alpha\beta} - \chi_{\beta\alpha}) = -2\text{Im}(\chi_{\alpha\beta}) = i \langle 0 | [\mathcal{A}_\alpha, \mathcal{A}_\beta] | 0 \rangle \quad (5.8)$$

But from this point on we would mostly focus on $g_{\alpha\beta}$ as it gives new Geometric Invariant named Euler Characteristics to identify Phases and Phase Transitions in our desired system. Since this prescription is independent of detail of any model, we can use it across wide range of quantum many body systems to gather a geometric perspective of its phases - therefore for the sake of cataloguing our fundamental concepts in theoretical science, we may call it the Phase Geometry (of a many-body system).

5.2 Ground state manifold (GSM)

This new geometric insight emerged due to the pioneering works of Zanardi *et al.* [5] beginning with Critical Scaling of Quantum Geometric Tensor and it interestingly elucidates

- How a distance captures the statistical distinguishability of quantum states: Lesser the overlap $|\langle \psi | \phi \rangle|$ between 2 states in the Hilbert Space, further they are in the distance (w.r.t the standard \mathcal{L}^2 -Norm) within the Hilbert Space - and therefore more statistically distinguishable. Had the ground state remained almost itself under small change of parameters i.e. when $\mathcal{F}(\lambda, \lambda + \delta\lambda) \rightarrow 1$ the line element $ds^2 \rightarrow 0$, therefore nothing statistically distinguishable would have happened in classically observing the system after this tiny parameter sweep. The main picture in the geometric approach to Quantum Phase Transitions is that - Near the critical point, small changes in the parameters usually make dramatic changes in the ground state. Also recalling from (5.6) that the geometric tensor is invariant under any local phase transformation in the parameter space - meaning the phase gathered in an adiabatic evolution with not affect the Phase Geometry - we can see that it truly captures the non-Adiabatic effects in Many-Body Quantum Systems [1].
- How singularities of the curvature of a manifold associated with the parameter space of a system can uniquely correspond to Quantum Phase Transitions therein providing “a universal conceptual framework to study quantum critical phenomena which is differential geometric and information theoretic at the same time.” [5]

- How in the case of finite temperature a statistical distance is linear to the specific heat at leading order in the change of temperature - Using (*Uhlmann fidelity*), a measure of fidelity in finite temperature, the authors have reported

$$\mathcal{F}_{Uhlmann}(\beta, \beta + \delta\beta) \sim \exp[-c_V(\beta) \frac{\delta\beta^2}{\beta^2}] \implies ds^2 \sim \frac{c_V(\beta)}{\beta^2} d\beta^2 \quad (5.9)$$

Which is “...remarkable in that it connects the distinguishability degree of two neighboring thermal quantum states directly to the macroscopic thermodynamical quantity c_V .”[5]

5.2.1 Intrinsic geometry of quantum phases of matter

Given a real differential manifold \mathcal{M} a collection of transition maps $\{\phi_\alpha : U \subset \mathcal{M} \rightarrow V \subset \mathbb{R}^n\}$ exists that makes \mathcal{M} locally homeomorphic¹ to open subsets of \mathbb{R}^n for some n . Distances can be defined on it by endowing upon it a metric that smoothly assigns a second rank bilinear and symmetric tensor $g_p : T_p\mathcal{M} \times T_p\mathcal{M} \mapsto \mathbb{R}$ on the tangent space $T_p\mathcal{M}$ that satisfies all the conditions of an inner product. Riemann generalized Gauss’s work of *Theorema Egregium* on higher dimensional smooth manifolds than just 2 to conclude that Scalar Curvature and Curvature Tensors do not depend on the Parameterization of the Manifold, and capture the local information of the geometry in terms of intrinsic coordinates. Using that, global information about the manifold’s geometry can be computed which are robust against smooth variable transformation of the parameters - therefore the curvature and geometric invariants we obtain are intrinsic to the models that can be obtained for arbitrary functional dependence of the parameters in the theory.

The Euler Characteristics of a (possibly) open manifold \mathcal{M} is an integer equal to the integrated Gaussian Curvature over the entire manifold with an additional boundary term [1] [3] :

$$\xi(\mathcal{M}) = \frac{1}{2\pi} \left(\int_{\mathcal{M}} K dS + \int_{\partial\mathcal{M}} k_g dl \right) = 2 - 2g \quad (5.10)$$

A standard notation for the Euler Characteristics is χ , but because we used that for denoting the geometric tensor $\xi(\mathcal{M})$ would be our notation for Euler Characteristics where g measures the number of holes in the case of closed manifold. The two terms in the above equation are the bulk and boundary contributions to the Euler Characteristics of the manifold which we distinguish as :

$$\xi_{bulk}(\mathcal{M}) = \frac{1}{2\pi} \int_{\mathcal{M}} K dS \quad \& \quad \xi_{boundary}(\mathcal{M}) = \int_{\partial\mathcal{M}} k_g dl \quad (5.11)$$

As the bulk and boundary Euler Integrals. These quantities, along with their constituents - the Gaussian Curvature (K), the Geodesic Curvature (k_g), the Area Element (dS), the area element (dl) - are geometric invariants, meaning that they remain unmodified under any change of variables. The used jargon for is is that - these quantities are Diffeomorphism Invariants of \mathcal{M} - meaning which are preserved under any diffeomorphism² of the the manifold

To simplify our analysis we will look at the geometry in the 2-dimensional cuts in the parameter space, so that we can use formulas for computing the Gaussian Curvature. For concrete calculations it would be convenient to stick to one set of formulas, which we will consider from Chapter IV and V from [6], and in particular *Theorem 46.1*. So the tools we need for our analysis are the following.

$$\text{Metric Determinant:} \quad g = \det[g_{ij}], \quad \& \quad \text{Line Element:} \quad ds^2 = Edu^2 + Fdudv + Gdv^2 \quad (5.12)$$

$$\text{Gaussian Curvature:} \quad K = \frac{R_{1212}}{g}, \quad (5.13)$$

¹A continuous bijection

²a smooth bijection

$$\text{Scalar Curvature: } R = g^{ab} R_{acb}^c = g^{ab} Ric_{ab} = g^{ab} (g_{ab} K) = \dim(\mathcal{M}) K$$

$$\text{Geodesic Curvature: } k_g = -\Gamma'_{22} \frac{\sqrt{g}}{G^{\frac{3}{2}}} \quad \text{where} \quad \Gamma' \equiv \Gamma(u_1 = \text{fixed value}; u_1 = 0) \quad (5.14)$$

$$\text{Area Element: } \sqrt{g} d\lambda_1 d\lambda_2, \quad \& \quad \text{Line Element: } dl = \sqrt{G} d\lambda_2 \quad (5.15)$$

Note the expression of k_g using Theorem 49.1 and Expression 49.8a from [6], when u_1 is kept constant, gives us the equivalent curve for Phase Boundary for $h = 1$. Also dl is given for a curve of constant λ_1 and g^{ij} is the inverse metric - and the Christoffel Symbols of the First Kind Γ_{bc}^a and the completely covariant Riemann Curvature Tensor R_{abcd} , in the $\{h, \gamma, \phi\}$ space are given by:

$$\Gamma_{bc}^a = \frac{1}{2} g^{ad} (\partial_c g_{bd} + \partial_b g_{cd} - \partial_d g_{bc}) \quad \& \quad R_{abcd} = g_{ak} (\partial_c \Gamma_{db}^k - \partial_d \Gamma_{cb}^k + \Gamma_{ce}^k \Gamma_{db}^e - \Gamma_{de}^k \Gamma_{cb}^e) \quad (5.16)$$

Although the analytic expression of this Curvature scalars are cumbersome they are unique functions of the components of the metric tensor in any choice of coordinate. An advantage of this geometric way of looking at it, is that singularities in the curvature cannot be removed by any reparameterization or coordinate transformation in the parameter space, and therefore intrinsic to the manifold the distances change dramatically under small displacement on it near the critical point/singularity. Therefore following [5], the statistical distinguishability varies rapidly under small parameter sweeps near those singularities - meaning classical observations would yield different qualitative behaviors of the Ground State of the System. This is how a Quantum Phase Transition is perceived geometrically. Therefore such a framework can reveal that it is not the choice of the parameters but their symmetries in a particular model, that plays its role in the spectrum and also in its critical behavior.

5.2.2 Ground state manifold of XYTF model

Continuing our journey through the phases of a Quantum XY Spin Chain using (??) and (5.7) and equipped with enough motivation and tools, we present the concrete Phase Geometry of this model across different 2 dimensional cuts in detail, where the complete *all-in-one* form is still absent covering every part of the parameter space simultaneously. So our parameter space is :

$$\{h, \gamma, \phi : -\infty \leq h, \gamma \leq \infty, -\pi \leq \phi \leq \pi\}$$

And the nonzero components of the geometric tensor, calculated using $g_{\alpha\beta} = \frac{1}{2} \langle 0 | \{ \mathcal{A}_\alpha \mathcal{A}_\beta | 0 \} \rangle_c$ are

$$g_{hh} = \frac{1}{4} \sum_k (\partial_h \theta_k)^2, \quad g_{\gamma\gamma} = \frac{1}{4} \sum_k (\partial_\gamma \theta_k)^2, \quad g_{h\gamma} = g_{\gamma h} = \frac{1}{4} \sum_k (\partial_h \theta_k)^2, \quad \& \quad g_{\phi\phi} = \frac{1}{4} \sum_k \sin^2(\theta_k) \quad (5.17)$$

$$\text{Where: } \partial_h \theta_k = -\frac{\gamma \sin k}{((h - \cos k)^2 + \gamma^2 \sin^2 k)}, \quad \partial_\gamma \theta_k = \frac{\sin k (h - \cos k)}{((h - \cos k)^2 + \gamma^2 \sin^2 k)}, \quad \& \quad (5.18)$$

$$\sin^2(\theta_k) = \frac{\gamma^2 \sin^2 k}{((h - \cos k)^2 + \gamma^2 \sin^2 k)}$$

It is possible to compute the metric tensors for finite systems using this discrete sum, but in the thermodynamic limit $L \rightarrow \infty \implies d(k \sim \frac{1}{L}) \rightarrow 0 \implies \sum_k \rightarrow \frac{L}{4\pi} \int_{-\pi}^{\pi}$ so that we can obtain analytic expressions of the geometric tensor of this model. Now these integrals can be evaluated by observing that e^{ik} makes $-\pi, \pi$ a closed curve, or the unit circle centered at origin of the Complex Space which we define to be our contour of integration \mathcal{C} . Therefore complexifying our momentum i.e.

$$k \in \mathbb{R} \rightarrow k \in \mathbb{C} \text{ by } k \mapsto z = e^{ik} \implies dk = \frac{dz}{iz} \quad \& \quad \int_{-\pi}^{\pi} dk \rightarrow \oint_{\mathcal{C}} \frac{dz}{iz}, \quad (5.19)$$

Now using $\sinh k = \frac{1}{2i}(z - \frac{1}{z})$ & $\cosh k = \frac{1}{2}(z + \frac{1}{z})$ that the integrals for our components of the metric tensor take the form

$$g_{hh} = \frac{i\gamma^2}{4\pi(-1+\gamma)^2(1+\gamma)^2} \oint_{\mathcal{C}} dz \frac{z(z^2-1)^2}{((z-z_1^+)(z-z_1^-)(z-z_2^+)(z-z_2^-))^2}, \quad (5.20)$$

$$g_{\gamma\gamma} = \frac{i}{16\pi(-1+\gamma)^2(1+\gamma)^2} \oint_{\mathcal{C}} dz \frac{(z^2+1-2hz)^2(z^2-1)^2}{z((z-z_1^+)(z-z_1^-)(z-z_2^+)(z-z_2^-))^2} \quad (5.21)$$

$$g_{h\gamma} = \frac{i\gamma}{8\pi(-1+\gamma)^2(1+\gamma)^2} \oint_{\mathcal{C}} dz \frac{(z^2+1-2hz) \cdot (z^2-1)^2}{((z-z_1^+)(z-z_1^-)(z-z_2^+)(z-z_2^-))^2} \quad (5.22)$$

$$g_{\phi\phi} = \frac{i\gamma^2}{16\pi(1-\gamma)(1+\gamma)} \oint_{\mathcal{C}} dz \frac{(z^2-1)^2}{z((z-z_1^+)(z-z_1^-)(z-z_2^+)(z-z_2^-))} \quad (5.23)$$

With the poles given as:

$$z_1^{\pm} = \frac{h \mp \sqrt{h^2 + \gamma^2 - 1}}{1 - \gamma}, \quad z_2^{\pm} = \frac{h \pm \sqrt{h^2 + \gamma^2 - 1}}{1 + \gamma}, \quad \& \quad z_0 = 0 \quad (5.24)$$

Where in evaluating the integral all we need to take care of is which of these poles are inside our contour, so that whenever the denominator contains z , i.e. for the cases of $g_{\gamma\gamma}$ and $g_{\phi\phi}$ the simple pole at $z_0 = 0$ anyway exists but non-triviality arises when we want to derive the conditions when the absolute values of the poles are less than or equal to 1. So to systematize evaluating these integrals, we plot [in Fig 6.] the regions of (h, γ) when each of the poles have absolute value ≤ 1 , shaded in blue. We can clearly see nice symmetry, induced by the functional form of the poles which allow us to consider 4 different possibilities for our nontrivial poles.

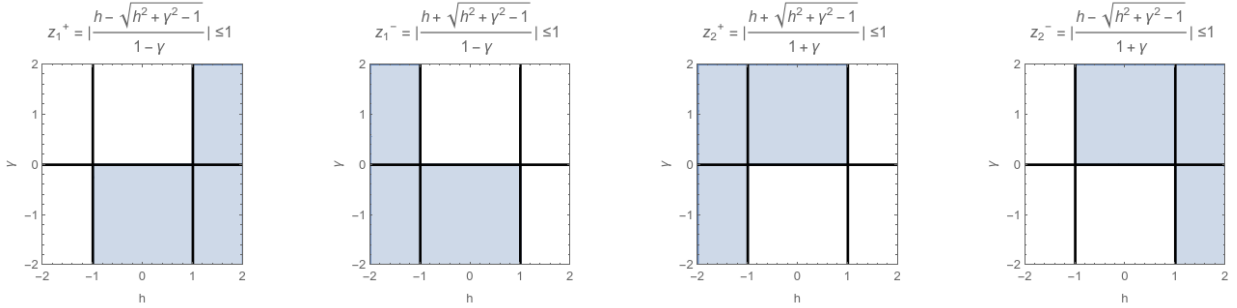


Figure 5.2: non-trivial poles in the integrands of geometric tensor components when $L \rightarrow \infty$

$$\begin{aligned} \mathbf{1.} \gamma \geq 0 \ \& \ |h| < 1 \implies \{z_2^+, z_2^-\} \quad \mathbf{2.} \gamma \leq 0 \ \& \ |h| < 1 \implies \{z_1^+, z_1^-\}, \\ \mathbf{3.} h > 1 \implies \{z_1^+, z_2^-\} \quad \mathbf{4.} h < -1 \implies \{z_1^+, z_2^+\} \end{aligned} \quad (5.25)$$

So keeping track of the nature of the poles, which sometimes are simple and other times of second order - we have evaluated them in the following table. It is of utmost importance that the nature of these poles determine the analytic expression of the systems susceptibilities - and the symmetry of the Phase Diagram of this model bear extreme resemblance with the symmetry of the conditions for the poles being inside the contour, in Fig. 6. So now with the information of the metric at hand we can look for Geometric Invariants in the system. Note also, when $\gamma = 1$ our initial theory (4.1) becomes Transverse Field Ising Model (denoted by brown solid line in the Phase Diagram, Fig. 5) - which we proceed to analyze in detail.

$ h < 1$	Metric Components	$ h > 1$
$\frac{1}{16} \frac{1}{ \gamma (1-h^2)}$	g_{hh}	$\frac{1}{16} \frac{ h \gamma^2}{(h^2-1)(h^2+\gamma^2-1)^{\frac{3}{2}}}$
$\frac{1}{8} \frac{ \gamma }{ \gamma +1}$	$g_{\phi\phi}$	$\frac{1}{8} \frac{\gamma^2}{1-\gamma^2} \left(\frac{ h }{\sqrt{h^2+\gamma^2-1}} - 1 \right)$
$\frac{1}{16} \frac{1}{ \gamma (1+ \gamma)^2}$	$g_{\gamma\gamma}$	$\frac{1}{16} \frac{2 h ^3-2h^2\sqrt{-1+h^2+\gamma^2}-2(-1+\gamma^2)\sqrt{-1+h^2+\gamma^2}+ h (-2+\gamma^2+\gamma^4)}{(-1+\gamma^2)^2(-1+h^2+\gamma^2)^{3/2}}$
0	$g_{h\gamma}$	$\frac{1}{16} \frac{- h \gamma}{h(h^2+\gamma^2-1)^{\frac{3}{2}}}$
0	$g_{h\phi}, g_{\gamma\phi}$	0

TFIM : $(h - \phi)$ plane for $\gamma = 1$

Using the metric above we want to know the isometric surface for the $(h - \phi)$ cut when $\gamma = 1$ whose coefficient in the fundamental form are our metric components. So the non-zero components, and thus coefficients of the first fundamental form are now

$$E = g_{hh}^{\gamma=1} = \begin{cases} \frac{1}{16(1-h^2)} & \text{if } |h| < 1 \\ \frac{1}{16h^2(h^2-1)} & \text{if } |h| > 1 \end{cases} \quad \& \quad G = g_{\phi\phi}^{\gamma=1} = \begin{cases} \frac{1}{16} & \text{if } |h| < 1 \\ \frac{1}{16h^2} & \text{if } |h| > 1 \end{cases} \quad (5.26)$$

Note here that for evaluating $g_{\phi\phi}(\gamma = 1)$ when $|h| > 1$, the expression in the table is useless as it says the metric diverges at $\gamma = 1$, instead look at the original expression of (5.17) and evaluate directly from it, by putting $\gamma = 1$ in it, then the above result will be obtained. Further observe that, the overall global angle or rotation ϕ around z -axis doesn't change the spectrum, and therefore should not affect the Phases - meaning the level surface of this metric in (h, ϕ) coordinates will have invariance along ϕ and therefore the surface will have cylindrical symmetry [as no other 2D surface has complete angular invariance]. Furthermore we can represent the 2-dimensional surface as its 3-dimensional embedding, so parameterizing our shape in cylindrical coordinates and requiring that -

$$dz^2 + dr^2 + r^2 d\phi^2 = g_{hh}^{\gamma=1} dh^2 + g_{\phi\phi}^{\gamma=1} d\phi^2 \quad (5.27)$$

$$\implies r(h) = \sqrt{g_{\phi\phi}^{\gamma=1}}, \quad \& \quad z(h) = \int_0^h dx \sqrt{g_{hh}^{\gamma=1}(x) - \left(\frac{dr(x)}{dx}\right)^2}$$

$$\text{Giving: } r(h, \phi) = \begin{cases} \frac{1}{4} & \text{if } |h| < 1 \\ \frac{1}{4|h|} & \text{if } |h| > 1 \end{cases} \quad \& \quad z(h, \phi) = \begin{cases} \frac{1}{4} \sin^{-1}(h) & \text{if } |h| < 1 \\ \frac{\pi|h|}{8h} + \frac{\sqrt{h^2-2}}{h} & \text{if } |h| > 1 \end{cases}$$

Notice an interesting subtlety in evaluating $z(h, \phi)$ when $|h| > 1$, putting (5.26) into the formula for the cylinder's height we get:

$$z(h, \phi) = \frac{1}{4} \begin{cases} \sin^{-1}(1) + \int_1^h \frac{dx}{x^2(\sqrt{x^2-1})} & \text{if } h > 1 \\ \sin^{-1}(-1) + \int_{-1}^h \frac{dx}{x^2(\sqrt{x^2-1})} & \text{if } h < -1 \end{cases} \quad (5.28)$$

$$\frac{v=\frac{\sqrt{x^2-1}}{x}}{\text{substitute}} \rightarrow \frac{1}{4} \begin{cases} \left. \frac{\sqrt{x^2-1}}{x} \right|_1^h + \frac{\pi}{2} & \text{if } h > 1 \\ \left. \frac{\sqrt{x^2-1}}{x} \right|_{-1}^h - \frac{\pi}{2} & \text{if } h < -1 \end{cases} = \frac{\pi|h|}{8h} + \frac{\sqrt{h^2-1}}{4h}$$

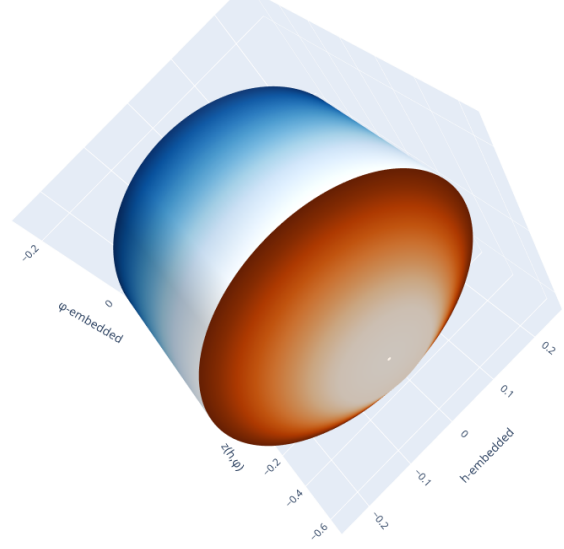
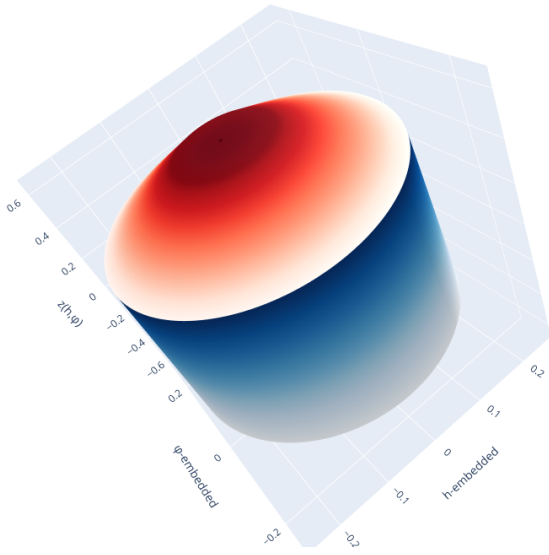


Figure 5.3: for $|h| < 1$ [Blue], & $h > 1$ [Red] Figure 5.4: for $|h| < 1$ [Blue], & $h < -1$ [Orange]

Which has been plotted in Fig. 7. Note here the axis of the cylinder is the h and the angular coordinate is the ϕ , so that when $|h| < 1$ (blue) the ferromagnetic phase is represented by uniform cylinder with flat geometry, and the 2 paramagnetic phases cap that cylinder from $|h| = 1 \rightarrow |h| = \infty$ in both the signs. These surfaces have strictly positive constant curvature. Computing the curvature scalars give us respectively 0 & 16 for the Ferromagnetic and Paramagnetic Phases.

$$K = \begin{cases} 0 & \text{if } |h| < 1 \equiv \text{Ferromagnetic} \\ 16 & \text{if } |h| > 1 \equiv \text{Paramagnetic} \end{cases} \quad \& \quad \xi_{bulk} = \begin{cases} \xi_{bulk}^{|h|<1} = 0 & \text{if } |h| < 1 \equiv \text{Ferromagnetic} \\ \xi_{bulk}^{|h|<1} = 1 & \text{if } |h| > 1 \equiv \text{Paramagnetic} \end{cases} \quad (5.29)$$

Therefore computation of the Bulk Euler Characteristics will obviously give 0 for the Ferromagnetic $|h| < 1$ case, but for Paramagnetic case we find

$$\xi_{bulk}^{|h|<1} = 0 \equiv \xi_{bulk}^{FM}, \quad \& \quad \xi_{bulk}^{h>1} = \frac{1}{2\pi} \int 16\sqrt{g} \, dh \, d\phi = \int_1^\infty dh \frac{1}{h^2\sqrt{h^2-1}} = 1 = \xi_{bulk}^{h<-1} = \xi_{bulk}^{PM} \quad (5.30)$$

Therefore the total Euler Characteristics of the surface would be 2, which is same as that of a Sphere, as this shape is homeomorphic to a closed surface without any hole in it. With this, we conclude our discussion on Phase Geometry of the Transverse Field Ising Model, and proceed computing the geometry of the full model in different cuts, and find the peculiar nature of the singularities.

Note that, topology of this Geometry has nothing to do with whether the Phase Transition in the underlying model is topological or not - this is just a smooth representation of the statistical distinguishability of the ground state wavefunctions, and its global properties captures the invariants under adiabatic deformations.

XY : $(\gamma - \phi)$ plane $\forall h$

Restricting our analysis of local distinguishability of ground states in the parameter space when the magnetic field is kept at a fixed value h , we can use the previous ansatz of cylindrical symmetry to

obtain the parameterization of one embedding that captures the same intrinsic distance relations as the metric components $\{g_{\gamma\gamma}, g_{\gamma\phi}, g_{\phi\phi}\}$ when regarded as the first fundamental form of that surface. The appearance of the functions may be intimidating but they are all C^∞ , and when required they can be evaluated numerically.

$$dz^2 + dr^2 + r^2 d\phi^2 = g_{\gamma\gamma} d\gamma^2 + g_{\phi\phi} d\phi^2 \implies r(\gamma, \phi) = \sqrt{g_{\phi\phi}}, \quad \& \quad z(\gamma, \phi) = \int_0^\gamma dx \sqrt{g_{\gamma\gamma}(x) - \left(\frac{dr(x, \phi)}{dx}\right)^2} \quad (5.31)$$

would give us the parameterization of an embedding in the form $\{r \cos\phi, r \sin\phi, z\}$ where the functions evaluated are the following.

$$\text{Gives: } r(\gamma, \phi) = \begin{cases} \sqrt{\frac{\gamma}{8+8\gamma}} & \text{if } |h| < 1 \\ \frac{1}{\sqrt{8(1-\gamma^2)}} \sqrt{\gamma^2(-1 + \frac{h}{\sqrt{-1+h^2+\gamma^2}})} & \text{if } |h| > 1 \end{cases}, \quad \& \quad \text{when: } |h| < 1 : \quad (5.32)$$

$$z(\gamma, \phi) = \frac{\sqrt{\gamma} \sqrt{\frac{1+2\gamma}{\gamma(1+\gamma)^3}} \left(\sqrt{\gamma}(1+\gamma) + \frac{i(1+\gamma)^{3/2} (\text{EllipticE}(i \sin^{-1}(\sqrt{\gamma}), 2) - \text{EllipticF}(i \sin^{-1}(\sqrt{\gamma}), 2))}{\sqrt{1+2\gamma}} \right)}{2\sqrt{2}}, \quad (5.33)$$

But when: $|h| > 1$ the integral cannot be evaluated analytically but only numerically. Due to its immensely long shape we are not reporting the function here for the sake of brevity.

Here the elliptic integrals of first ($\text{EllipticF} \equiv F(\phi|m)$) and second ($\text{EllipticE} \equiv E(\phi|m)$) kinds respectively are defined as :

$$F(\phi|m) = \int_0^\phi \frac{1}{\sqrt{1-m\sin^2(\theta)}} d\theta, \quad \& \quad E(\phi|m) = \int_0^\phi \sqrt{1-m\sin^2(\theta)} d\theta$$

The corresponding embeddings are:

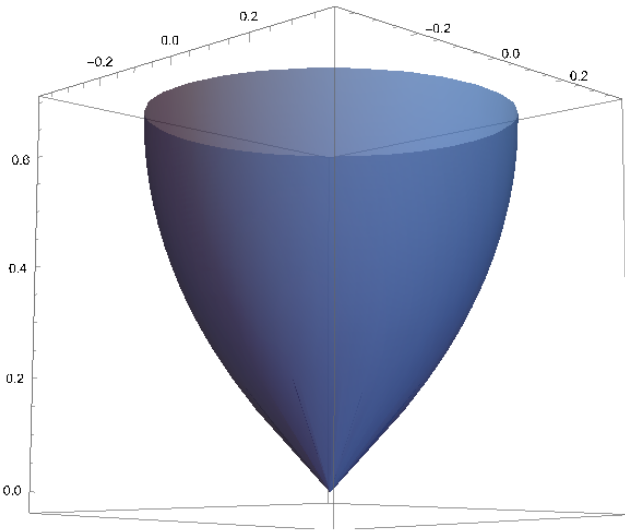


Figure 5.5: $(\gamma - \phi)$ plane when $|h| < 1$

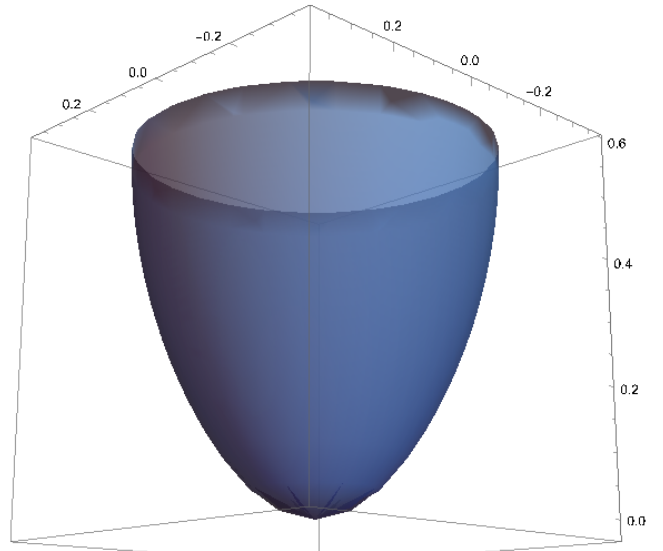


Figure 5.6: $(\gamma - \phi)$ plane when $|h| > 1$

It is interesting to observe that the case when $|h| < 1$, the *ground state manifold* contains a conical singularity at $\gamma = 0$, corresponding to anisotropic phase transition as the spectrum of the theory becomes gapless at that point, whereas when $|h| > 1^3$, we do not observe any singularity at

³Note that the embedding of the ground state manifold presented have been numerically evaluated with $h = 1.01$

$\gamma = 0$, which can also be explained with the singularity of the gaussian curvature of the $(\gamma - \phi)$ plane. This explains once again the phase diagram of the full theory, i.e. the $\gamma = 0$ is the point of phase transition as long as the magnitude of the transverse magnetic field does not exceed 1. Moreover the *bulk-Euler characteristics* do indeed characterise the phase transition between the ferromagnetic and paramagnetic phases of the theory.

$$K_{(\gamma-\phi)} = \begin{cases} 4 & \text{if } |h| < 1 \equiv \text{FM} \\ \frac{4(\sqrt{h^2+\gamma^2-1}(8h^4+8(\gamma^2-1)+h^2(-16+8\gamma^2+\gamma^4))+(-2+\gamma^2+\gamma^4)(-2h+2h^3)-2h^3+4h^5)}{\sqrt{h^2+\gamma^2-1}(4+4h^4-4\gamma^2+h^2(-8+4\gamma^2+\gamma^4))} & \text{if } |h| > 1 \equiv \text{PM} \end{cases} \quad \& \quad (5.34)$$

$$\xi_{bulk, (\gamma-\phi)} = \begin{cases} = \xi_{bulk}^{|h|<1} = \frac{1}{\sqrt{2}} & \text{if } |h| < 1 \equiv \text{FM} \\ = \xi_{bulk}^{|h|>1} = \xi_{bulk}^{h<1} + \xi_{bulk}^{h<-1} = 1 + 1 = 2 & \text{if } |h| > 1 \equiv \text{PM} \end{cases} \quad (5.35)$$

Which rightly justifies that the information-dynamics in both the 2 phases are qualitatively distinct, as the global geometric invariant is evidently so.

$(h - \gamma)$ plane $\forall \phi$

The richness of the ground state manifold is most prominent in the case of $(h - \gamma)$ cut where we know that unlike ϕ , h and γ do change the spectrum of the theory where ϕ only modifies the ground state phase. The case when $|h| > 1$, the embeddings cannot be obtained by any conventional method because only the 2 dimensional metric tensor does not guarantee any embedding of a surface in 3 dimensional euclidean space that carries the exact same intrinsic distance relations as captured in the second fundamental form with coefficients $\{g_{\gamma\gamma}, g_{\gamma h}, g_{hh}\}$. One requires the coefficients of the second fundamental form that encapsulates the extrinsic curvature of the surface w.r.t. the embedding space, as well as compatibility in *Gauss-Codazzi-Mainardi Equations* followed by solving the frame equation - which guarantees existence and uniqueness of the solutions as long as the second fundamental form and first fundamental form are compatible [6]. Nevertheless the route is ill-defined in our context with only the metric components at hand - since the initial conditions of various partial differential equations cannot be obtained with the *adiabatic gauge potentials*. The fact that the previous embeddings could be found is the consequence of reasonable ansatz but one may obtain many embeddings or surfaces in \mathbb{R}^3 for a given second fundamental form.

Conformal Flatness: One embedding can be solved directly from the line-element for $|h| < 1$ that captures the most essential physics. Moreover one can use the metric tensor of the ground state manifold and its eigenspectrum to define protocols⁴ such that the net excitations out of the ground state is extremised following the integral curves of the eigenvectors of the metric tensor from any given non-singular point. But the interesting feature of this manifold is its conformal flatness that further elucidates the notion of statistical distinguishability. The geometric tensor for $|h| < 1$ is given by:

$$g = \begin{pmatrix} \frac{1}{16} \frac{1}{|\gamma|(1-h^2)} & 0 \\ 0 & \frac{1}{16} \frac{1}{|\gamma|(1+|\gamma|)^2} \end{pmatrix} \implies ds^2 = \frac{1}{64} \frac{1}{|\gamma|} d\tilde{s}^2 \implies \tilde{g} = \begin{pmatrix} \frac{4}{(1-h^2)} & 0 \\ 0 & \frac{4}{(1+|\gamma|)^2} \end{pmatrix} \quad (5.36)$$

⁴curves in the parameter space

Where g is conformal to \tilde{g} with the conformal factor of $\frac{1}{64|\gamma|}$ ⁵. Note that a 3D embedding of this conformal ground-state manifold can be obtained directly from the line element as :

$$d\tilde{s}^2 = \frac{4}{(1-h^2)} dh^2 + \frac{4}{(1+|\gamma|)^2} d\gamma^2 = d(2\sin^{-1}(h))^2 + d(2\log(1+|\gamma|))^2$$

Which already indicates flatness, meaning invariant-statistical-distinguishability across that specific range of parameters ($|h| < 1$). Furthermore note that both the coordinates are angular function so consider a radius of $r(\bar{h}, \bar{\gamma}) = 1$ and \bar{h} as the angular variable of a cylinder so that the \tilde{g} can be represented as:

$$\begin{aligned} d\tilde{s}^2 &= d\bar{h}^2 + d\bar{\gamma}^2 = d\bar{r}^2 + r^2 d\bar{h}^2 + d\bar{\gamma}^2 \implies \text{Embedding: } \{\cos(\bar{h}), \sin(\bar{h}), \bar{\gamma}\} \\ &\equiv \{\cos(2\sin^{-1}(h)), \sin(2\sin^{-1}(h)), 2(\log(1+|\gamma|))^2\} \end{aligned}$$

That gives us an open cylinder with radius 1 and height $4\tan^{-1}(\sqrt{|\gamma|})$ which is clearly a manifold of 0 curvature and is represented in 5.7.

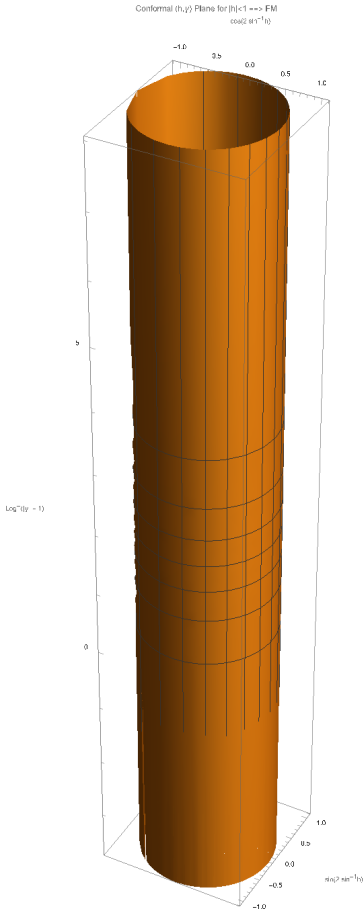


Figure 5.7: Conformally Flat $(h-\gamma)$ -cut for $|h| < 1$

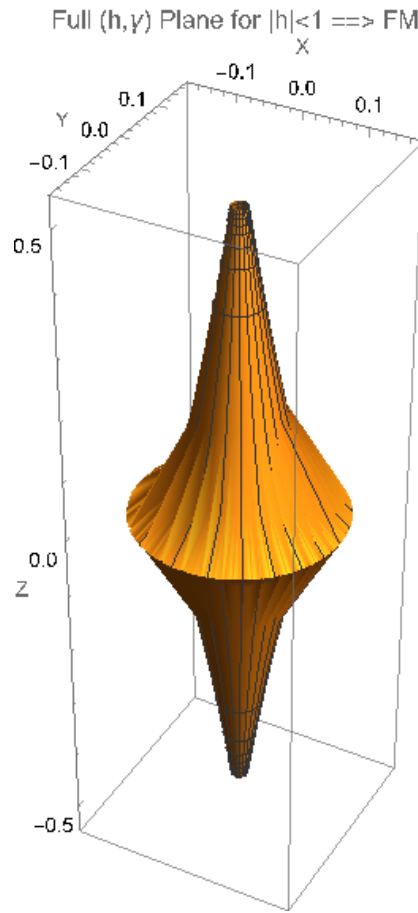


Figure 5.8: Exact $(h-\gamma)$ -cut for $|h| < 1$

Exact Ground State Manifold: for $|h| < 1$ can be solved by observing the line element and harnessing cylindrical symmetry:

$$ds^2 = \frac{1}{16\gamma(1-h^2)} dh^2 + \frac{1}{16\gamma(1+|\gamma|)^2} d\gamma^2 \quad (5.37)$$

⁵the rationale to keep a $\frac{4}{(1-h^2)}$ term is to consider it as an angular variable in a way that $h \in [-1, 1] \mapsto \bar{h} \in [-\pi, \pi]$ without loss of generality

$$= \left(\frac{1}{8\sqrt{\gamma}}\right)^2 d(2\sin^{-1}(h))^2 + \frac{d\gamma^2}{256\gamma^3} + dz^2 = r^2 d\phi^2 + dr^2 + dz^2$$

which can be completely determined by solving for $z(h, \gamma)$ to get:

$$z(h, \gamma) = \int \sqrt{\frac{(5\gamma+1)(3\gamma-1)}{256\gamma^3(1+\gamma)^2}} d\gamma$$

$$= \frac{1}{8} \text{Re} \left[\frac{1}{-5-10\gamma+75\gamma^2} \sqrt{75-\frac{5}{\gamma^2}-\frac{10}{\gamma}\gamma^{\frac{5}{2}}(1+\gamma)} \sqrt{\frac{-1-2\gamma+15\gamma^2}{\gamma^3(1+\gamma)^2}} \times \left(5\text{EllipticE} \left[\sin^{-1} \left(\frac{1}{\sqrt{3}\sqrt{\gamma}} \right), -\frac{3}{5} \right] \right. \right.$$

$$\left. \left. -4 \left(\text{EllipticF} \left[\sin^{-1} \left(\frac{1}{\sqrt{3}\sqrt{\gamma}} \right), -\frac{3}{5} \right] + 4\text{EllipticPi} \left[-3, \sin^{-1} \left(\frac{1}{\sqrt{3}\sqrt{\gamma}} \right), -\frac{3}{5} \right] \right) \right) \right]$$

So that we can construct **one embedding** for the ground state manifold for $|h| < 1$ as 5.8:

$$\text{Embedding: } \left\{ \frac{1}{8\sqrt{|\gamma|}} \cos(2\sin^{-1} h), \frac{1}{8\sqrt{|\gamma|}} \sin(2\sin^{-1} h), \bar{z}(h, \gamma) \right\}, \quad (5.38)$$

$$\text{with: } \bar{z}(h, \gamma) = \begin{cases} z(h, \gamma) & \text{if } \gamma > 0, \\ -z(h, \gamma) & \text{if } \gamma < 0 \end{cases}$$

Where the elliptic integrals of first ($\text{EllipticF} \equiv F(\phi|m)$), second ($\text{EllipticE} \equiv E(\phi|m)$) and third ($\text{EllipticPi} \equiv \Pi(n; \phi|m)$) kinds respectively defined as :

$$F(\phi|m) = \int_0^\phi \frac{1}{\sqrt{1-m\sin^2(\theta)}} d\theta, \quad E(\phi|m) = \int_0^\phi \sqrt{1-m\sin^2(\theta)} d\theta, \quad \&$$

$$\Pi(n; \phi|m) = \int_0^\phi \frac{\sqrt{1-m\sin^2(\theta)}}{1-n\sin^2(\theta)} d\theta$$

The scalar curvature can be computed for the phase to be $K = -\frac{8}{|\gamma|}(1+|\gamma|)$ with curvature singularity $\gamma = 0$ corresponding to the anisotropic phase transition that connects the fact that in the full XY chain in transverse field, $\gamma = 0$ is a critical line as long as $|h| < 1$. It is already known that *Gabriel's horn* or otherwise known as *Torricelli's trumpet*⁶ which has strictly negative curvature, resembles the same shape when we restrict either sign of anisotropy γ there the surface area diverges as $\gamma \rightarrow 0$ which is clear from divergence of the radius of the cylinder $r = \frac{1}{8\sqrt{\gamma}}$. Note that the ansatz of cylindrical symmetry will not save us in the last cut of $(h - \gamma)$ plane with $|h| > 1$.

When $|h| > 1$ the the components of the metric do not admit any known ansatz due to the presence of cross-term, and the nature of the function. It is given by:

$$g = \begin{pmatrix} E & F \\ F & G \end{pmatrix} \quad \text{with: } E = \frac{h\gamma^2}{(h^2-1)(h^2+\gamma^2-1)^{\frac{3}{2}}}, \quad F = -\frac{\gamma}{(h^2+\gamma^2-1)^{\frac{3}{2}}}$$

$$\& \quad G = \frac{2h^3 - 2h^2\sqrt{-1+h^2+\gamma^2} - 2(-1+\gamma^2)\sqrt{-1+h^2+\gamma^2} + h(-2+\gamma^2+\gamma^4)}{(-1+\gamma^2)^2(-1+h^2+\gamma^2)^{3/2}}$$

And the scalar curvature $K = \left(1 + \frac{|h|}{\sqrt{h^2+\gamma^2-1}}\right)$ doesn't diverge anywhere in the whole parameter region of $\{|h| > 1, \forall \gamma\}$. It is worth noting that, in general the solution of a parameterization in any \mathbb{R}^n from the second-fundamental form along, is not possible. To guarantee an embedding one requires

⁶3D embedding of a surface with strictly negative curvature contains within, a finite volume with infinite surface area. It is the surface of revolution of $y = \frac{1}{x}$ about the x -axis.

the first-fundamental form as well as compatibility condition of coefficients of both the fundamental forms in the Codazzi-Mainardi Equations, which is a set of coupled first order PDE. That compatibility guarantees the existence and solution of Frame Equations, which in turn guarantees an unique parameterization. Since this only explains the lack of a complete embedding of this last cut we refer to [6] for further discussions as this is an *inverse problem*, whereas concrete surface to metric is the route usually analysed. Further note that the qualitative change of the scalar curvature for $|h| < 1$ and $|h| > 1$ fits with the hypothesis under investigation.

5.2.3 Scalar curvature and Euler-characteristics of XYTF

Following the idea that the curvature singularities of this geometric tensor or the metric constructed out of fidelity susceptibilities - uniquely correspond to the critical points and phases transitions, the table below shows how the gaussian curvature associated with all the 2-dimensional cuts in the following table, and plots.

$ h \leq 1$	Gaussian Curvature ($K = R_{1212}/g$)	$ h > 1$
0	TFIM $\equiv (h, \phi)$ at $\gamma = 1$	16
0	$(h, \phi) \forall \gamma$	$4 \left(1 + \frac{1-\frac{1}{\gamma^2}}{h^2} + \frac{1}{\gamma^2} + \frac{2 h }{\sqrt{-1+h^2+\gamma^2}} \right)$
$-\frac{8}{ \gamma } (1 + \gamma)$	$(h, \gamma) \forall \phi$	$8 \left(1 + \frac{ h }{\sqrt{h^2+\gamma^2-1}} \right)$
4	$(\gamma, \phi) \forall h$	a long C^∞ function, but ignored for brevity

Where the first 3 of the scalar curvatures corresponds to each of the 2-dimensional cuts and the last one corresponds to the full 3-dimensional ground state manifold. As is clear from the diagrams, there is always a discontinuity at the second order phase transition $h = \pm 1$ and for the first order phase transition at $\gamma = 0$ we find either discontinuity or divergence. The complete meaning of this quantity still remains to investigate further; but it sure encapsulates the information content in the excitations above the ground state quite elegantly.

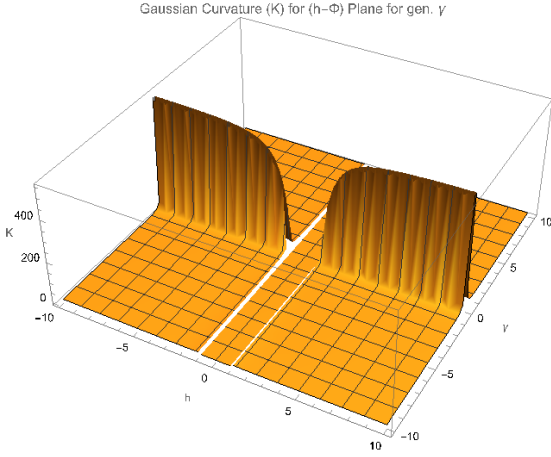
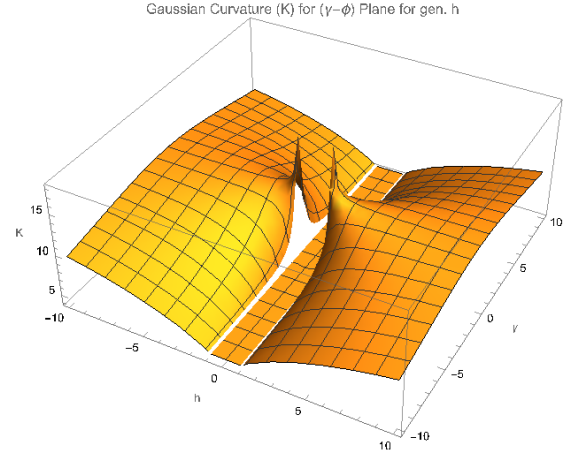
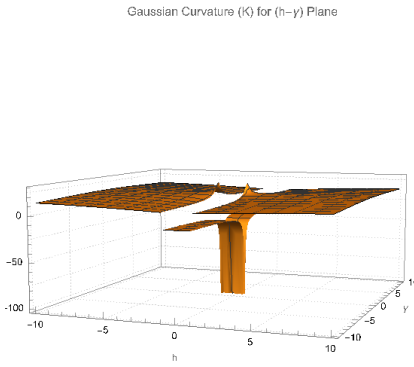
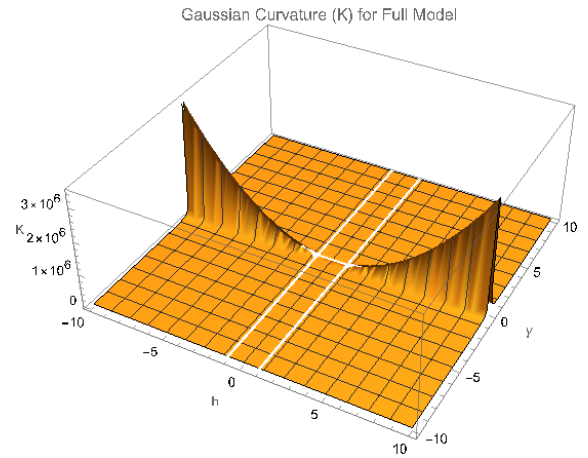
Similarly the *Bulk Euler Characteristics* (5.11) will be able to distinguish the different Phases in this 0-temperature Quantum Many-Body system.

$ h \leq 1$	Bulk Euler Characteristics $[\xi_{bulk}(\mathcal{M}) = \frac{1}{2\pi} \int_{\mathcal{M}} K dS]$	$ h > 1$
0	TFIM $\equiv (h, \phi)$ at $\gamma = 1$	1 [when $h > 1$] + 1 [when $h < -1$]
0	$(h, \phi) \forall \gamma$	1 [when $h > 1$] + 1 [when $h < -1$]
$\frac{1}{\sqrt{2}}$	$(\gamma, \phi) \forall h$	1 [when $h > 1$] + 1 [when $h < -1$]

Reflecting the global conservation of a geometric invariant across a quantum phase.

5.2.4 Discussions

Note that: one can determine the exact metric components, fidelity-susceptibility and also complete embeddings for slices of the parameter space - strictly due to exact solvability of the underlying theory.


Figure 5.9: K for $(\phi - h)$ Plane for fixed γ

Figure 5.10: K for $(\phi - \gamma)$ Plane for fixed h

Figure 5.11: K for $(h - \gamma)$ Plane

Figure 5.12: K for the full parameter space

The adiabatic gauge potential computed from the wavevector-space and transformed in the real-space is exact, and therefore captures the variation of the system's excitation-amplitudes exactly; both away and near the critical points. Otherwise one would require the variational principle described above to determine *best-local approximations* of the adiabatic gauge potential, which would inevitably fail to capture the systems behaviour near any gapless point. This **limitation of the application of adiabatic gauge potential** motivates to investigate different geometric measures of the information content in a quantum many-body system. The next chapter explores one such quantity inspired from Information Geometry.

The interesting perspective⁷ it brings is that *corresponding to any evolution of a smoothly parameterized distribution*, one can endow a non-euclidean metric on the parameter space that encapsulates the *distinguishability of the distributions* at different parameter values. In this context, the meaning of - number of distinguishable states between two measurements of states prepared at different parameter values - have been established by Woiters in [7], which is the distance measured with this endowed metric at two different parameter points. Using metric as a generalized distance, there have been many efforts to have a smooth assignment of *how different two distributions are*, as one varies the parameters. This gives one way of putting the information content of some random process into a geometry of the underlying parameter space. But the choice may not be unique, as any quantity (say B) derived from some quantity (say A) that is related to the system's states for small change of parameters, which is

⁷I speculate it to be true but to the best of my knowledge there is no rigorous result backing it.

Consider A to be a smoothly assigned quantity relating two states at infinitesimally varying parameters, and B , a quantity derived from A that is a symmetric, positive rank-2 tensor. Since B satisfies all the properties of a riemannian metric it may be considered one. But there may be many A s and correspondingly B s, but interesting would be to check the dependency of B or the information-content on the choice of A when there can be more than one such A s.

In the context of Quantum Information, the fidelity-susceptibility is the starting point of deriving a geometry of the ground state manifold. Here $A_1(\vec{\lambda}|\vec{\delta\lambda}) = 1 - \mathcal{F}(\lambda, \lambda + \delta\lambda)$ and $B_1 = g_{\alpha\beta} = \frac{1}{2}\langle 0|\{\mathcal{A}_\alpha\mathcal{A}_\beta|0\rangle_c$ and the route followed due to 1) the positivity of A_1 , and 2) an extrema of A_1 as $\delta\lambda \rightarrow 0$, so that the leading contribution of the parameters in A_1 are quadratic. Now considering $\vec{\lambda} \equiv \{\lambda_i\}$ to be the coordinates the total variation of A_1 between $\vec{\lambda}$ and $\vec{\lambda} + \vec{\delta\lambda}$ can be approximated by the arc-length of a curve as $A_1(\vec{\lambda}|\vec{\lambda} + \vec{\delta\lambda}) \approx ds^2(\vec{\lambda}) = g_{\alpha\beta}(\vec{\lambda}) d\lambda^\alpha d\lambda^\beta$. Where the picture completed by thinking the parameter space as a curved manifold and evolution of the system amounts to trajectory of a point particle on it, where locally $g_{\alpha\beta}$ is a local measure of how distinguishable two distributions are on the manifold. It follows the diagonal components are the susceptibilities of A_1 for different parameters as it measures how sensitive A_1 is under variation of some λ_i .

This idea can be generalised to obtain an infinite class of riemannian metric tensors to give a measure of how sensitive the entangled-ordering is w.r.t. the parameters, in a many-body quantum system.

* — *

Chapter 6

A susceptibility of entanglement-entropy

It is known that the Fisher-Rao information metric (g^{FR}) locally approximates the Kullback-Leibler divergence (D_{KL}) in the following way

$$D_{KL}(p_\lambda||q_\lambda) = \int d\lambda \ p_\lambda \ln\left(\frac{p_\lambda}{q_\lambda}\right) \implies \text{when: } q_\lambda = p_{\lambda+\delta\lambda} \approx p_\lambda + d\lambda^i \frac{\partial p_\lambda}{\partial \lambda^i} \ , \quad (6.1)$$

$$\implies \text{at } \mathcal{O}(d\lambda^2): \ D_{KL}(p_\lambda||p_{\lambda+\delta\lambda}) = \left(\frac{1}{2} \int d\lambda \ p_\lambda \frac{\partial \ln(p_\lambda)}{\partial \lambda^i} \frac{\partial \ln(p_\lambda)}{\partial \lambda^j}\right) d\lambda^i d\lambda^j = g_{ij}^{FR} d\lambda^i d\lambda^j \quad (6.2)$$

Where both these two quantities are widely used in countless contexts, except in the study of a quantum phase transition. There is a quantum version of D_{KL} known as the Relative Entanglement Entropy $S(\hat{\rho}||\hat{\sigma})$ defined as:

$$S(\hat{\rho}||\hat{\sigma}) = \text{Tr}[\hat{\rho} \ln(\frac{\hat{\rho}}{\hat{\sigma}})] \quad (6.3)$$

that is one measure of how distinguishable two density matrices $\hat{\rho}$ and $\hat{\sigma}$ are, or in other words, the average uncertainty associated with measurements considering $\hat{\sigma}$ to be density matrix, where $\hat{\rho}$ is the actual one. The physical interpretation of entanglement, entropy are already estranged by speculation, so instead of attempting a physical interpretation, its positive-definiteness will be harnessed immediately. Note that when $\hat{\sigma}_\lambda = \hat{\rho}_{\lambda+\delta\lambda}$

$$\hat{\rho}_{\lambda+\delta\lambda} = \hat{\rho}_\lambda + \delta\lambda^i \partial_i \hat{\rho} \equiv \hat{\rho} + g, \text{ where: } g = \delta\lambda^i \partial_i \hat{\rho} \quad (6.4)$$

$$\implies \ln(\hat{\rho}_{\lambda+\delta\lambda}) \approx \ln(\hat{\rho} + g) \approx \ln(\hat{\rho}) + \rho^{-1}g - \frac{1}{2}\hat{\rho}^{-2}g^2, \text{ gives:}$$

$$S(\hat{\rho}_\lambda||\hat{\rho}_{\lambda+\delta\lambda}) \approx \text{Tr} [\hat{\rho} (-\hat{\rho}^{-1}g + \frac{1}{2}\hat{\rho}^{-2}g^2)] \quad (6.5)$$

$$= -d\lambda^i \cancel{\partial_i \text{Tr}[\hat{\rho}]} + \frac{1}{2} \text{Tr} [\hat{\rho} \partial_i(\ln \hat{\rho}) \partial_j(\ln \hat{\rho})] d\lambda^i d\lambda^j = \Xi_{ij} d\lambda^i d\lambda^j$$

$$\text{where: } \boxed{\Xi_{ij} = \frac{1}{2} \text{Tr}[\hat{\rho} \partial_i(\ln \hat{\rho}) \partial_j(\ln \hat{\rho})]} \quad (6.6)$$

That satisfies all the properties of a riemannian metric, and as is evident, $S(\hat{\rho}_\lambda||\hat{\rho}_{\lambda+\delta\lambda}) \geq 0$ and equality holds when $\delta\lambda \rightarrow 0$, which is its minima. Therefore in this context $A_2 \equiv S(\hat{\rho}_\lambda||\hat{\rho}_{\lambda+\delta\lambda})$ giving $B_2 \equiv \Xi_{ij}$ can as well be another measure of the information content associated with entanglement-entropy of a quantum system, encapsulated into a geometry on the parameter space. Moreover the diagonal components measure the variation of $S(\hat{\rho}_\lambda||\hat{\rho}_{\lambda+\delta\lambda})$ across any fixed parameter, giving a susceptibility of Entanglement-Entropy. We now demonstrate the behaviour of Ξ_{hh} and $\Xi_{\gamma\gamma}$ for the XY Spin Chain in Transverse Magnetic Field where γ is the anisotropy and h is the transverse magnetic field.

6.1 Exact results for XY spin chain in transverse magnetic field :

Consider again the model under investigation

$$\mathcal{H} = - \sum_{j=1}^L \left(\left(\frac{1+\gamma}{2} \right) \sigma_j^x \sigma_{j+1}^x + \left(\frac{1-\gamma}{2} \right) \sigma_j^y \sigma_{j+1}^y + h \sigma_j^z \right) \quad (6.7)$$

with the definitions as laid out before. Now we require a density matrix than is easy to compute but gives sufficient information about the systems entanglement. Since the order parameter in this theory is the expectation of single-body operator, the single body reduced density matrix $\hat{\rho}^{(1)} = \text{Tr}_{(\text{all except } i)} [\hat{\rho}]$ and due to translational symmetry, this is same for all sites i . Using operator product expansion we know

$$\hat{\rho}^{(1)} = \frac{1}{2} (\mathbb{I}_{2 \times 2} + \sum_{\alpha \in \{x,y,z\}} \text{Tr}[\hat{\rho} \hat{\sigma}^\alpha] \hat{\sigma}^\alpha), \quad \text{with the full density matrix: } \hat{\rho} = \frac{e^{-\beta \hat{\mathcal{H}}}}{\text{Tr}[e^{-\beta \hat{\mathcal{H}}}]}$$

In our context, $\beta \rightarrow \infty$ as we are looking at $T \rightarrow 0$, purely quantum state, with no thermal activity. Now we will focus the analysis on the finite systems, which indicate the convergence to the critical point of the system when $N \rightarrow \infty$ very rapidly even for very small system size and estimate its scaling for 2 different models, Transverse Field Ising model and XY model.

Note that the hamiltonian possesses the following symmetry : $\{\hat{\sigma}^x \rightarrow -\hat{\sigma}^x, \hat{\sigma}^y \rightarrow -\hat{\sigma}^y, \hat{\sigma}^z \rightarrow \hat{\sigma}^z\}$, which is also maintained by the ground state of every finite system, except only the one with infinitely many spins. This makes expectation of $\hat{\sigma}^x$ and $\hat{\sigma}^y$ identically vanish in any finite system, leaving us with [8]:

$$\hat{\rho}^{(1)} = \frac{1}{2} (\mathbb{I}_{2 \times 2} + m_z \hat{\sigma}^z) , \quad \text{where: } m_z(h, \gamma) = \langle \sigma^z \rangle \quad (6.8)$$

We now compute m_z for arbitrary system size starting with the diagonalization of the hamiltonian which would give an effective quasiparticle picture of the excitations above the ground state which can be performed by spinless Bogolioubov fermions. Following the Jordan-Wigner transformation and going to the momentum space as Eq. (4.2) one finds :

$$\mathcal{H} = - \sum_k \Psi_k^\dagger \begin{pmatrix} (h - \cos k) & -\gamma \sin k e^{i\phi} \\ -\gamma \sin k e^{-i\phi} & -(h - \cos k) \end{pmatrix} \Psi_k = \sum_k \epsilon_k \gamma_k^\dagger \gamma_k + \text{Const} \quad (6.9)$$

$$\text{with: } \Psi_k = \begin{pmatrix} c_k \\ c_{-k}^\dagger \end{pmatrix} = \begin{pmatrix} \cos \frac{\theta_k}{2} & i \sin \frac{\theta_k}{2} \\ i \sin \frac{\theta_k}{2} & \cos \frac{\theta_k}{2} \end{pmatrix} \begin{pmatrix} \gamma_k \\ \gamma_{-k}^\dagger \end{pmatrix}, \quad (6.10)$$

$$\theta_k = \tan^{-1} \left(\frac{\gamma \sin k}{h - \cos k} \right), \quad \& \quad \epsilon_k = \pm \sqrt{(h - \cos k)^2 + \gamma^2 \sin^2 k}$$

Here $\{\gamma_k^\dagger, \gamma_k\}$'s are the creation and annihilation operators of the Bogolioubov fermions. Therefore the hamiltonian diagonalizes in the number operator basis of these Bogolioubov fermions where excitations in each of the momentum-mode costs ϵ_k amount of energy and γ_k annihilates excitations from the ground state of each of those momentum modes, therefore the correct ground state is not the one annihilated by c_k but of γ_k . This ground state, the generalized spin-ful version of which is the BCS ground state is given as :

$$|0\rangle = \bigotimes_k \left(\cos \frac{\theta_k}{2} - \sin \frac{\theta_k}{2} c_k^\dagger c_{-k}^\dagger \right) |0_k\rangle, \quad \text{such that: } \langle 0|0\rangle = 1, \quad \& \quad \gamma_k |0\rangle = 0 \quad (6.11)$$

$$\text{using: } \sigma_i^z = 1 - 2 c_i^\dagger c_i, \quad \text{so that: } m_z = \frac{1}{L} \sum_i \langle \sigma_i^z \rangle \quad (6.12)$$

$$\begin{aligned}
 &= \frac{1}{L} \sum_i \left[\langle 0|0 \rangle - 2 \langle 0| \left(\sum_{k_1 k_2} c_{k_1}^\dagger c_{k_2} e^{ir_i(k_1-k_2)} \right) |0 \rangle \right] = 1 - \frac{2}{L} \sum_k \langle 0| c_k^\dagger c_k |0 \rangle \\
 \text{now: } &\langle 0| c_k^\dagger c_k |0 \rangle = \bigotimes_{l, m} \langle 0_l | \left(\cos \frac{\theta_l}{2} - \sin \frac{\theta_l}{2} c_{-l} c_l \right) [c_k^\dagger c_k] \left(\cos \frac{\theta_m}{2} - \sin \frac{\theta_m}{2} c_m^\dagger c_{-m} \right) |0_m \rangle \\
 &= \langle 0_k | \left(\cos \frac{\theta_k}{2} - \sin \frac{\theta_k}{2} c_{-k} c_k \right) c_k^\dagger c_k \left(\cos \frac{\theta_k}{2} - \sin \frac{\theta_k}{2} c_k^\dagger c_{-k} \right) |0_k \rangle = \sin^2 \frac{\theta}{2} = \frac{1}{2} (1 - \cos \theta_k)
 \end{aligned}$$

Since the momentum modes contribute in the whole spectrum as tensor product of unentangled states for each of the modes each of the operators only act on corresponding states labeled by that momentum and under inner product with itself, all other modes except k becomes 1 due to normalization condition satisfied by

$$\langle 0_l | \left(\cos \frac{\theta_l}{2} - \sin \frac{\theta_l}{2} c_{-l} c_l \right) \left(\cos \frac{\theta_l}{2} - \sin \frac{\theta_l}{2} c_l^\dagger c_{-l}^\dagger \right) |0_l \rangle = \cos^2 \frac{\theta_l}{2} + \sin^2 \frac{\theta_l}{2} = 1 \quad (6.13)$$

$$\text{therefore: } m_z = 1 - \frac{2}{L} \sum_k \frac{1}{2} (1 - \cos(\theta_k)) = \frac{1}{L} \sum_k \frac{h - \cos k}{\sqrt{(h - \cos k)^2 + \gamma^2 \sin^2 k}}$$

More explicitly, Having L equidistant angles (momentum modes) within $[-\pi, \pi]$ requires

$$m_z(h, \gamma, L) = \frac{1}{L} \sum_{l=-(\frac{L-1}{2})}^{l=(\frac{L-1}{2})} \frac{h - \cos(\phi_l)}{\sqrt{(h - \cos(\phi_l))^2 + \gamma^2 \sin^2(\phi_l)}}, \quad \text{with: } \phi_l = \frac{2\pi l}{L} \quad (6.14)$$

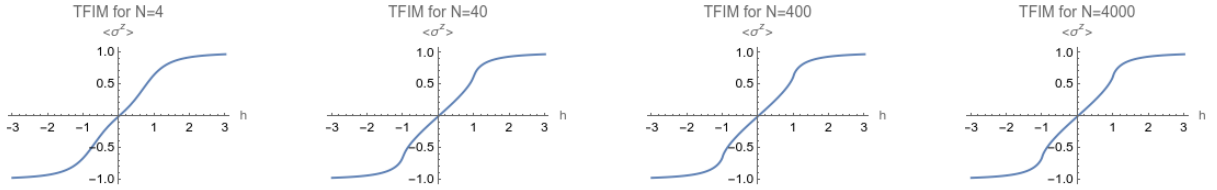


Figure 6.1: Examples of $\langle \sigma^z \rangle$ for different system sizes when $\gamma = 1$

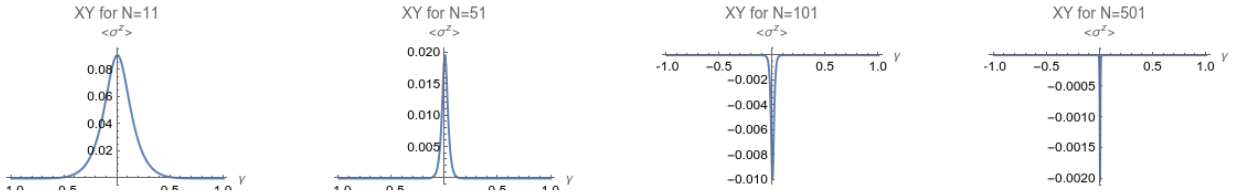


Figure 6.2: Examples of $\langle \sigma^z \rangle$ for different system sizes when $h = 0$

This completes the analytic expression for $\hat{\rho}^{(1)}$ that we can compute for any finite system size as defined in Eq. (6.8). We are now ready to compute the susceptibility of entanglement-entropy of two systems at two different limits of this hamiltonian.

$$\text{For XY model: } \boxed{\chi_L^{XY} = \Xi_{\gamma\gamma}^{(h=0)}(L)}, \quad \& \quad (6.15)$$

$$\text{For transverse field Ising model : } \boxed{\chi_L^{TFIM} = \Xi_{hh}^{(\gamma=1)}(L)}$$

Note the choice of even number of spins for TFIM and odd number of spins for XY model. When $\gamma = 1$, taking odd system size in Eq (6.14) inevitably gives a $k = 0$, which corresponds to $(h - 1)$ in the denominator, hitting one of the thermodynamic critical points, something that we will avoid by restricting to only even system sizes for TFIM. But for XY model, i.e. when $h = 0$, the summand becomes $g(\phi_l) = \frac{-\cos(\phi_l)}{\sqrt{\cos^2(\phi_l) + \gamma^2 \sin^2(\phi_l)}}$, which has the property that $g(\pi - \phi_l) = -g(\phi_l)$ so that

for even spins, momentum modes for either $[0, \pi]$ and $[-\pi, 0]$ pairwise cancel, giving $m_z(0, \gamma, 2N) = 0$, \forall integer N . That is why everything remains well defined and non-trivial as long as we keep even system size for TFIM and odd system sizes for XY. One can derive well-defined riemannian metric tensors directly using Eq. (6.6) (6.14), and (6.8) to analyse the sensitivity of entanglement-entropy of the full theory in (h, γ) space, but we will focus on the specific limits in detail to estimate the scaling of its peaks' convergence to the thermodynamic critical point as the system size varies.

6.1.1 Signature of quantum criticality in finite XY model

The behaviour of χ_L^{XY} as defined in (6.15) has finite maxima for every finite system, and the peak of it approaches to the thermodynamic critical point with algebraic scaling. Not the expressions, but their behaviour is of more importance and keeping in mind that $\gamma_c^\infty = 0$ corresponds to that gapless point when the system is thermodynamically large one finds:

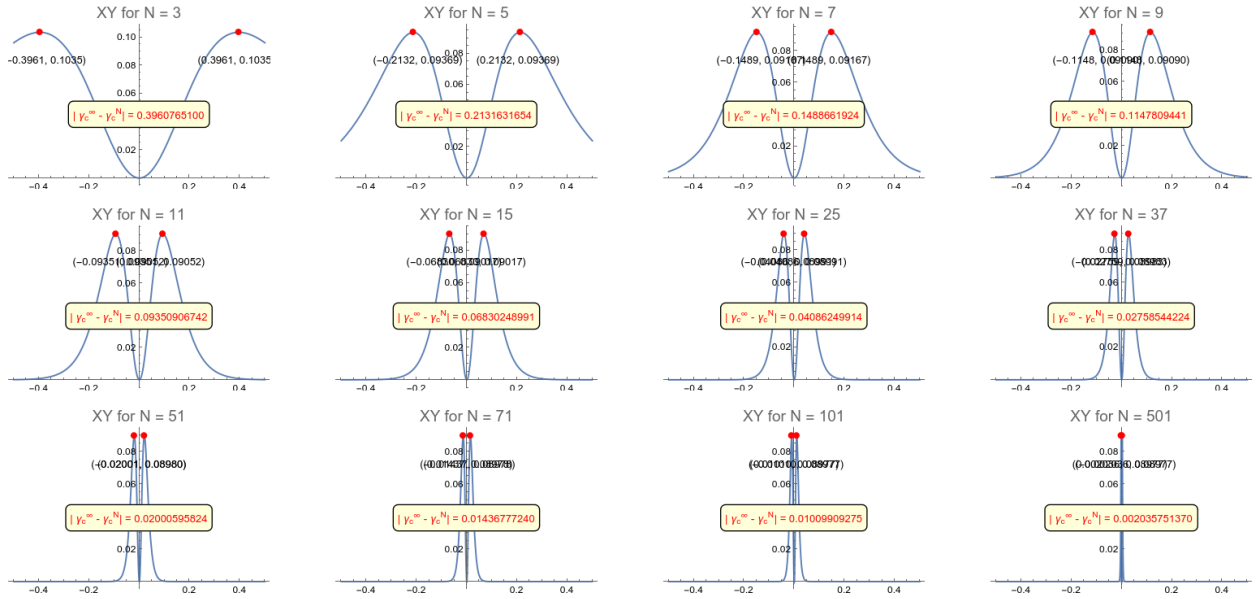


Figure 6.3: Susceptibility of Entanglement-Entropy $\Xi_{\gamma}^{(h=0)}$ for XY model

Not only the convergence of the peak to the true critical point, the narrowing of the susceptibility near the maxima strongly indicates strongest susceptibility near $\gamma = 0$ as the system size increases. In the log-log scale the distance from the thermodynamic critical point, and the maxima of this susceptibility shows:

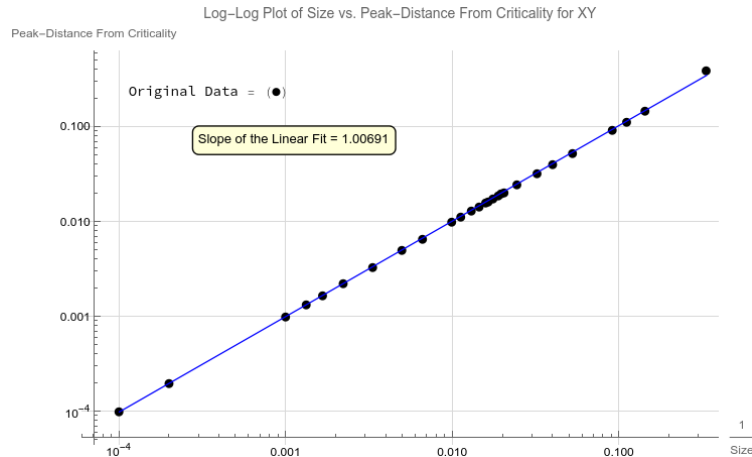


Figure 6.4: Scaling of $|\gamma_c^{L \rightarrow \infty} - \gamma_c^{\text{finite } L}|$ w.r.t. $\frac{1}{L}$ for XY model in the Log-Log scale

Which evidently gives $|\gamma_c^{L \rightarrow \infty} - \gamma_c^{\text{finite } L}| \sim \frac{1}{N}$, \forall odd integer N

6.1.2 Signature of quantum criticality in finite TFIM

The similar behaviour for χ_L^{TFIM} again rapidly converges to the thermodynamic critical point in the following way, while narrowing sharply near the critical points :

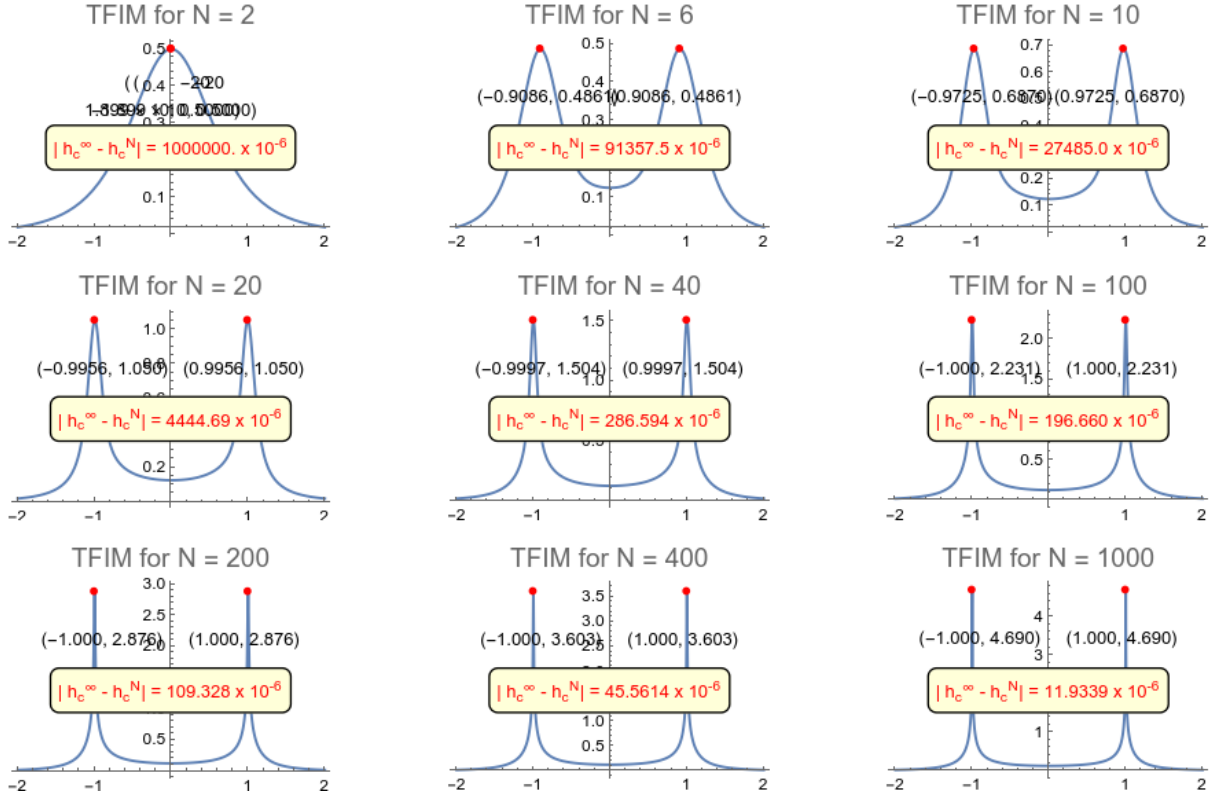


Figure 6.5: Susceptibility of Entanglement-Entropy $\Xi_{hh}^{(\gamma=1)}$ for Transverse Field Ising model

But the distance from its peak $|h_c^{L \rightarrow \infty} - h_c^{\text{finite } L}|$ at all the system sizes do not scale uniformly and something non-trivial happens near system size $N \sim 50$ where it scales exponentially w.r.t. $\frac{1}{N}$, therefore two different linear fit has been made to account for both kind of scaling:

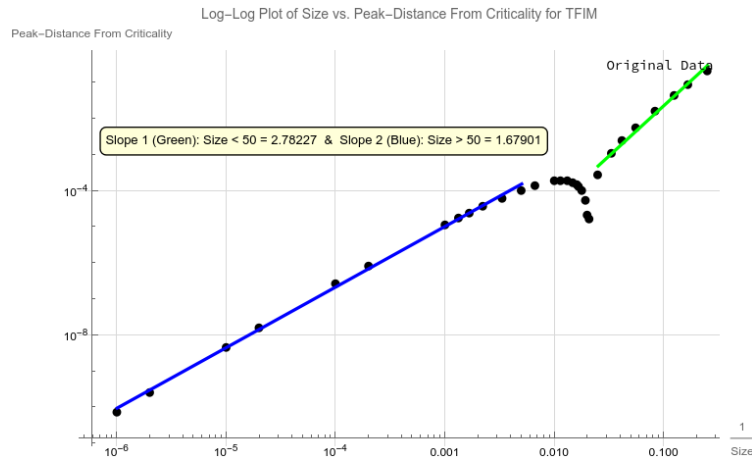


Figure 6.6: Scaling of $|h_c^{L \rightarrow \infty} - h_c^{\text{finite } L}|$ w.r.t. $\frac{1}{L}$ for Transverse Field Ising model in the Log-Log scale

Giving two different scaling behaviours, respectively as $|h_c^{L \rightarrow \infty} - h_c^{\text{finite } L}| \sim \frac{1}{N^{2.78}}$ when $N < 50$ and $|h_c^{L \rightarrow \infty} - h_c^{\text{finite } L}| \sim \frac{1}{N^{1.68}}$ when $N \gg 50$. Although it appeared numerical artifact it has been repeated but **not reproduced on other platforms** than Mathematica. This peculiarity is not understood yet.

It is worth noting that starting from a smooth function $m_z(h, \gamma, L)$ with no discontinuity or divergence at $h = \pm 1$ for all finite size systems, one obtains something that builds up only near those

points as $L \rightarrow \infty$. Also using Eq. (6.6) one can obtain an infinite class of riemannian metric tensors, and susceptibility of entanglement-entropy as its diagonal components for all kinds of density matrices, that encapsulates the distinguishability of information content in the entanglement. If any $\hat{\rho}$ is pure, it anyway vanishes.

* — *

Chapter 7

Summary and open ends

- Originated from the hamiltonian mechanics as the generator of canonical transformation, adiabatic gauge potentials generalise into the generator of adiabatic deformations of eigenstates; which can be identified as the reason behind transitions between energy levels in a complex quantum systems.
- This allows to identically eliminate the transitions by introduction of *counter-diabatic hamiltonian* that evolves the eigenstates of some hamiltonian, exactly; demonstrated with **transitionless Landau-Zener-Majorana-Majorana (LZMM) problem** where any classical spin trajectory can be achieved by infinitely many external magnetic fields without causing any precision. The magnetic field that drives the solution of LZMM exactly, without transitions is derived by solving a second order differential equation using parabolic cylinder functions.

- A variational principle derives the best local approximation of the adiabatic gauge potential, which opens new roads to achieve adiabatic evolution of states, but with rapid driving protocols. The nature of the AGP is demonstrated in the XY spin- $\frac{1}{2}$ chain in transverse magnetic field. The fact that we can get the exact adiabatic gauge potential of the theory, roots in exact solvability or integrability of the model. **It would be very interesting to see the role of adiabatic gauge potential in the case of non-integrable models.**

- The signature of quantum criticality that is captured by the fidelity susceptibility has been generalised to endow a riemannian metric on the parameter space which defines the **ground state manifold**. For most of the two dimensional cuts we managed to solve embeddings as surfaces in \mathbb{R}^3 from which the nature of the quantum phase transition is elegantly apparent. Alongside, the scalar curvature and euler characteristics capture uniquely the information of quantum phases of ferromagnet and paramagnet. Since the ansatz of cylindrical symmetry have been helpful due to vanishing off-diagonal metric components, it amounts to no help for solving an embedding of $(h - \gamma)$ plane when $|h| > 1$. Integrability conditions coming from Codazzi-Mainardi equations require information of the coefficients of first-fundamental form and suitable boundary conditions - which is absent in this context, leaving this as an ill-defined situation to guarantee any existence or let alone uniqueness of an embedding. Therefore **an embedding remains to be solved for $(h - \gamma)$ plane when $|h| > 1$.**

- A susceptibility of entanglement-entropy has been proposed that captures the signature of quantum criticality even for very small system sizes in both the transverse field Ising chain and XY chain. **It gives an infinite class of riemannian metric tensors encapsulating the information content of entanglement-entropy.** Its peak converges to the actual thermodynamic critical point with algebraic scaling w.r.t. the system-size - while narrowing its width. This extrapolates to a divergence of dirac-delta type in the thermodynamically large system. But **this scaling for the case of transverse field Ising model shows a peculiarity.** For system sizes < 50 it scales with different power-law coefficient than with systems sizes $>> 50$. Though the results have been obtained using Mathematica software, it remains to be tested using other numerical techniques to make sure it is not an artifact of the numerical processes underneath it.

Chapter 8

Conclusion

This report presents a comprehensive study of adiabatic gauge potentials (AGPs) in time-dependent quantum systems. The report adeptly explores the role of AGPs as generators of special canonical transformations, their application in counterdiabatic driving, and their utility in emulating adiabatic dynamics rapidly for effective quantum state manipulation.

Significantly, the work delves into the analytics of dissipationless protocols, establishing a connection between AGPs and Berry Phase, and develops a formula for calculating AGPs. Through a minimum action principle, it demonstrates a method for determining variational optimal AGPs, offering insights into transitionless and dissipationless drives.

The application of these concepts in controlling complex systems, notably in the context of the XY model, is elucidated. The report culminates in a detailed analysis of the Landau-Zener-Majorana problem and a transitionless Landau-Majorana-Zener model, providing a clear demonstration of the theoretical concepts in a practical scenario.

Most interestingly, connecting Information Theory and Geometry to gain more insights about Phases of Quantum Systems using Statistical Distinguishability and Fidelity Susceptibility - gives us a new land to explore non-adiabatic critical aspects of such many-body systems.

The potential for future research in this field is immense. The implications of AGPs in quantum computing, quantum chaos, and material science, especially in understanding and controlling quantum phase transitions, are profound. Further exploration into the optimization of AGPs in non-integrable systems and their role in quantum error correction could significantly advance our understanding and capabilities in quantum technologies.

Furthermore an infinite class of riemannian metric tensors have been derived to encapsulate the information content in the entanglement-entropy, where starting from any impure density matrix, one can analyse the sensitivity of entanglement entropy of any given system. It would be great to see its potential in its full glory.

* — *

Chapter 9

Prospects and future directions

Various windows it opens which craves immediate exploration, and in particular the following list scratches the surface of potential future progress:

- **Extension to Non-Integrable Systems:** Investigating the application of AGPs in non-integrable quantum systems, which may provide deeper insights into quantum dynamics and system control beyond integrable models.
- **Quantum Computing Applications:** Exploring the utilization of AGPs for quantum state preparation and manipulation in quantum computing, potentially enhancing the efficiency and fidelity of quantum algorithms.
- **Advancements in Quantum Thermodynamics:** Utilizing AGPs to control and optimize quantum thermodynamic cycles, potentially leading to the development of more efficient quantum heat engines and refrigerators.
- **Material Science and Condensed Matter Physics:** Applying the concept of AGPs to understand and control quantum phase transitions in materials, offering possibilities for discovering new states of matter and novel material properties.
- **Quantum Error Correction:** Investigating the role of AGPs in quantum error correction techniques, which could lead to more robust quantum computing and communication systems.
- **Experimental Realizations:** Focusing on experimental demonstrations of AGP-based protocols in various physical systems, such as cold atoms, trapped ions, and superconducting qubits, to bridge the gap between theory and practice.
- **Development of Variational Methods:** Enhancing variational methods for approximating AGPs in complex systems, potentially simplifying the implementation of counterdiabatic driving in practical scenarios.
- **Interdisciplinary Approaches:** Encouraging interdisciplinary research combining AGPs with fields like machine learning, aiming to discover novel methods for system control and optimization in quantum technologies.
- Explanation to different scaling behaviours in TFIM for system size less than and greater than 50, would reveal the reason of such peculiarity.

Bibliography

- [1] Michael Kolodrubetz, Dries Sels, Pankaj Mehta, Anatoli Polkovnikov : *Geometry and non-adiabatic response in quantum and classical system.*
- [2] M V Berry : *Transitionless quantum driving.*
- [3] Michael Kolodrubetz, Vladimir Gritsev, and Anatoli Polkovnikov : *Classifying and measuring geometry of a quantum ground state manifold.*
- [4] J. P. Provost, G. Vallee : *Riemannian structure on manifolds of quantum states.*
- [5] Paolo Zanardi, Paolo Giorda, and Marco Cozzini : *Information-Theoretic Differential Geometry of Quantum Phase Transitions.*
- [6] Erwin Kreyszig : *Differential Geometry.*
- [7] W. K. Wootters : *Statistical distance and Hilbert space.*
- [8] T. J. Osborne¹ and M. A. Nielsen : *Entanglement in a simple quantum phase transition.*